VICTOR BUONO DA SILVA BAPTISTA

PRESSURE DISTRIBUTION ON CENTER-PIVOT LATERAL LINES: COMPARATIVE RESULTS AND ENERGY CONSERVATION WITH A VARIABLE SPEED DRIVE

LAVRAS – MG

2019

VICTOR BUONO DA SILVA BAPTISTA

PRESSURE DISTRIBUTION ON CENTER-PIVOT LATERAL LINES:

COMPARATIVE RESULTS AND ENERGY CONSERVATION WITH A VARIABLE SPEED DRIVE

Thesis submitted for the degree of Doctor of Philosophy in Irrigation and Drainage Engineering, Water Resources Postgraduate Program, Federal University of Lavras, Brazil.

Prof. Dr. Alberto Colombo (UFLA)
Prof. Dr. Miguel Angel Moreno (UCLM)
Supervisors

LAVRAS – MG

Ficha catalográfica elaborada pelo Sistema de Geração de Ficha Catalográfica da Biblioteca Universitária da UFLA, com dados informados pelo(a) próprio(a) autor(a).

Baptista, Victor Buono da Silva.
Pressure Distribution on Center-Pivot Lateral Lines: Comparative Results and Energy Conservation with a Variable Speed Drive / Victor Buono da Silva Baptista. - 2019.
81 p. : il.

Orientador(a): Alberto Colombo.
Coorientador(a): Miguel Ángel Moreno.
Tese (doutorado) - Universidade Federal de Lavras, 2019.
Bibliografia.

1. Center pivot irrigation. 2. Pressure distribution. 3. Hydraulic model. I. Colombo, Alberto. II. Moreno, Miguel Ángel. III. Título.

VICTOR BUONO DA SILVA BAPTISTA

PRESSURE DISTRIBUTION ON CENTER-PIVOT LATERAL LINES:
COMPARATIVE RESULTS AND ENERGY CONSERVATION WITH A VARIABLE SPEED DRIVE

Thesis submitted for the degree of Doctor of Philosophy in Irrigation and Drainage Engineering, Water Resources Postgraduate Program, Federal University of Lavras, Brazil.

APROVED in December 20, 2019.

Dr. Alberto Colombo	Federal University of Lavras (UFLA)
Dr. Adriano Valentim Diotto	Federal University of Lavras (UFLA)
Dr. Míguel Ángel Moreno	University of Castilla La-Mancha (UCLM)
Dr. Luiz Antônio Lima	Federal University of Lavras (UFLA)
Dr. Lessandro Coll Faria	Federal University of Pelotas (UFPel)

Prof. Dr. Alberto Colombo (UFLA)
Prof. Dr. Miguel Angel Moreno (UCLM)
Supervisors

LAVRAS – MG
2019

DECLARATION

I hereby declare that this work has been originally produced by myself for this thesis and it has not been submitted for the award of a higher degree to any other institution. Collaborations with other researchers, as well as publications or submissions for publication are properly acknowledged throughout the document.

Victor Buono da Silva Baptista, Lavras, December 2019.

ACKNOWLEDGEMENTS

I would like to take this opportunity to first and foremost thank my family. My parents Beth and Rogério, my love Mariane, my brothers Thais and Fabio, and all my family, a deep respect and gratitude to the ones that made this happen, the ones that gave me strength, patience and bravery to finish this task.

I would like to express my eternal gratitude to my supervisors/friends: Alberto Colombo, Adriano Valentim Diotto and Miguel Ángel Moreno. Thank you very much for your guidance, teaching and support.

Besides my supervisors, I would like to thank my judge committee: Luiz Antônio Lima, Lessandro Coll Faria, Gilberto Coelho and Geraldo Magela Pereira for their encouragement and insightful comments.

A special thanks for Marcelo Ribeiro Viola, Fabio Ponciano de Deus, Livia Alves Alvarenga, Carlos Rogério de Mello, Jacinto Assunção Carvalho, Manoel Alves de Faria, Michael Silveira Thebaldi, Luis Fernando Coutinho, Luiz Gonsaga de Carvalho, Carlos Eduardo Silva Volpato, Sandro Pereira, Alessandro Vieira Velloso, Renato, Elvis, Luiza, Júlio, João and all friends from the Engineering Department and Water Resources Department (UFLA).

I would like to thank José Maria Tarjuelo for having received me very well in Albacete. As well as friends Renato Leandro, Bruno Lellis, Jesús Pardo, Juan Ignácio Córcoles, Rafael Gonzales Perea and Rocio Ballesteros from the Centro Regional de Estudios del Agua and Escuela Técnica Superior de Ingenieros Agronomos y de Montes de Albacete.

A special thanks for friends José Henrique, Thiago, Maurício, Reginaldo, Rafael Faria, Brenon, Glaucio, Pietros, Geovane Junqueira, Diego Marin, Rodrigo Balbi, Bruno Cortez, Lara Gazolla and all friends from the K-Zona republic for all their help, hard work and full availability when I most needed. Also, for greats friends Frederico Novelli, Luciana Wilhelm, Rodrigo Padovani, Paulo Henrique, Pedro Jipa and Luiz Passos, for the exceptional moments in Europe.

Thanks for everyone that somehow made this work possible!

Finally, I also recognize my gratitude to CAPES (Coordination of Improvement of Higher Education Personnel – Process number 88881.190146/2018-01) for their financial support and scholarships.

ABSTRACT

The use of variable speed drives to control irrigation pumping running speed is one of the strategies to reduce energy consumption of center pivot systems operating on undulating topography. By varying the frequency of the power supply as the lateral line rotates in the field, pivot point pressure may be adjusted in order to decrease the excess pressure that is dissipated by pressure regulators at each outlet. However, in order to reduce energy consumption of a center pivot system operating with a variable speed drive without compromising the center pivot water application uniformity, the pumping unit behavior, the digital elevation model of the irrigated field, and the pressure distribution along the lateral line must all be fully characterized. A detailed description of pressure distribution along a center pivot lateral line and adequate knowledge of the minimum pressure point position along the center pivot lateral are required in order to define strategies to reduce energy consumption in center pivots operating with a variable pumping running speed. In this sense, this research aimed to study the spatial distribution of pressure along center pivot lateral line in plots with variable topography, and to analyze the energy conservation promoted by using variable speed drives in center pivot pumping units. As described in article 1, pressure distributions along a center pivot lateral line determined by four different analytical models were compared to pressure distribution determined by numerical solutions provided by the EPANET hydraulic simulator. Several different lateral line configurations were considered in this study: lateral line with one and two pipe diameters, application of different gross irrigation depths per revolution time, different values of the pipe wall roughness coefficients, different values of the ground slope, and lateral lines operating with and without an end gun. For all different center pivot lateral line configurations considered, two different friction head loss equations were used: the Darcy-Weisbach equation, and the Hazen-Williams equation. Regardless of friction head loss equation considered, the estimates of head loss distribution obtained with the four analytical solutions were very similar to those calculated with the EPANET hydraulic simulator. These results indicate that the detailed description of the flow distribution along the center pivot lateral line that is required by the numerical method did not improve the accuracy of the head loss distribution. In addition, the tedious process of editing input files required by EPANET may be restricted for its use. In this sense, in article 2 the VSPM (Variable Speed Pivot Model) was developed to perform hydraulic and energy analyses of center pivot systems using the EPANET hydraulics engine. Besides improving the process of editing EPANET input files, this tool can determine, using any type of digital elevation model, the elevation of each tower for each angular position of the center pivot lateral line. It is also capable of simulating, in an accurate manner, the performance of the center pivot controlled with a VSD. The possible reduction in energy consumption with the use of a VSD was simulated for a center pivot system located in Albacete (Spain), in an irrigated area presenting a 15.3 m maximum topographic elevation difference. This simulation indicated that energy consumption with a VSD is 12.2% lower than the energy consumption observed with the commonly used fixed pumping running speed. This reduction in energy consumption correspond to a reduction of 2,821.47 € on energy consumption expenses.

Keywords: Center pivot irrigation. Pressure distribution. Head loss correction factor. Hydraulic model. Energy consumption. Variable pumping running speed.

RESUMO

O uso de inversores de frequência para controlar a velocidade de operação do bombeamento de irrigação é uma das estratégias para reduzir o consumo de energia em pivôs centrais que operam em áreas com topografia ondulada. Ao variar a frequência da fonte de alimentação à medida que a linha lateral gira no campo, a pressão do ponto de articulação pode ser ajustada para diminuir a pressão excessiva dissipada pelas válvulas reguladoras de pressão em cada saída. No entanto, para reduzir o consumo de energia de um pivô central que opera com um inversor de frequência sem comprometer a uniformidade da aplicação da água, o comportamento da unidade de bombeamento, o modelo digital de elevação da área irrigada e a distribuição de pressão ao longo da linha lateral devem ser totalmente caracterizados. Uma descrição detalhada da distribuição de pressão e o conhecimento adequado da posição do ponto de mínima pressão ao longo da linha lateral são necessários para definir estratégias para reduzir o consumo de energia em pivôs centrais que operam com uma velocidade de operação de bombeamento variável. Nesse sentido, esta pesquisa teve como objetivo estudar a distribuição espacial da pressão ao longo da linha lateral do pivô central em parcelas com topografia ondulada e analisar a conservação de energia promovida pelo uso de inversor de frequência em sua unidade de bombeamento. Conforme descrito no artigo 1, as distribuições de pressão ao longo de uma linha lateral do pivô central determinada por quatro diferentes modelos analíticos foram comparadas à distribuição de pressão determinada por soluções numéricas fornecidas pelo EPANET. Diversas configurações de linha lateral foram consideradas neste estudo: linha lateral com um e dois diâmetros de tubo, aplicação de diferentes lâminas de irrigação por tempo de giro, diferentes valores dos coeficientes de rugosidade da parede do tubo, diferentes valores da inclinação do terreno e linhas laterais operando com e sem canhão final. Para todas as diferentes configurações de linha lateral do pivô central consideradas, foram comparadas duas equações de perda de carga diferentes: a equação de Darcy-Weisbach e a equação de Hazen-Williams Os resultados mostraram que, independentemente da equação de perda de carga considerada, as quatro soluções analíticas apresentaram estimativas de valores de perda muito semelhantes aos calculados com o EPANET. Esses resultados indicam que a descrição detalhada da distribuição de vazão ao longo da linha lateral do pivô central exigida pelo método numérico não melhorou a precisão da distribuição de perda de carga. Além disso, o tedioso processo de edição dos arquivos de entrada exigido pelo EPANET pode ser uma restrição para o seu uso. Nesse sentido, no artigo 2, o VSPM (*Variable Speed Pivot Model*) foi desenvolvido para realizar análises hidráulicas e de energia de sistemas de irrigação do tipo pivô central usando o EPANET. Além de melhorar o processo de edição dos arquivos de entrada EPANET, esta ferramenta pode determinar, usando qualquer tipo de modelo digital de elevação, a elevação de cada torre para cada posição angular da linha lateral do pivô central. Também é capaz de simular, de maneira precisa, o desempenho do pivô central controlado com um inversor de frequência. A possível redução no consumo de energia com o uso de um inversor de frequência foi simulada para um pivô central localizado em Albacete (Espanha), em uma área irrigada com uma diferença máxima de elevação de 15,3 m. Esta simulação indicou que o consumo de energia com um inversor de frequência é 12,2% menor que o consumo de energia observado com a operação de bombeamento a velocidade fixa, permitindo uma economia próxima a 2.821,47 €.

Palavras-chave: Pivô central. Distribuição de pressão. Fator de correção da perda de carga. Modelo hidráulico. Consumo de energia. Velocidade variável de operação de bombeamento.

SUMARY

1st CHAPTER – GENERAL INTRODUCTION

1 GENERAL INTRODUCTION

A major global concern for the coming years will be the supply of food in quantity and quality to meet demands of an increasing world population that is foreseen to achieve 9.15 billion inhabitants by the year 2050 (ALEXANDRATOS; BRUINSMA, 2012; PEREIRA, 2017). Thus, increasing food production to meet this demand is a challenge for agricultural professionals and requires studies on techniques that increase production efficiency. Increasing efficiency in food production requires improving all production processes, including improving both water use efficiency and energy use efficiency of irrigation systems. Irrigated agriculture represents 16% of the world's cultivated area and expects to produce 44% of world food production by 2050 (ALEXANDRATOS; BRUINSMA, 2012; PEREIRA, 2017; WBCSD, 2014).

Sustainable use of water resources could be accomplished by improving irrigation systems, thereby reducing the amount of water required to satisfy crop water requirements. In this regard, technological developments in infrastructures of irrigation systems contribute to increase water use efficiency. However, according to Tarjuelo et al. (2015), in recent years, increases on irrigation systems water use efficiency have been associated to a significant increase on electric energy consumption of irrigation systems. Higher consumer demand, coupled with a lack of investment in the generation, transmission and distribution sectors have been slowing the increase on electric energy supply. In a scenario of slowing increase on electric energy supply and growing demand, electric energy cost has been increasing, forcing consumers to seek various forms of energy savings, including improving electric efficiency use.

Sprinkler irrigation systems represent around 11% (35 million hectares) of the total irrigated areas in the world. Within this method, the most outstanding systems are set systems, traveling guns, center pivots, and linear-moving laterals (KELLER; BLIESNER, 1990). With eight million hectares of irrigated area, the center pivot system represents 23% of the area irrigated by sprinkler systems (AQUASTAT, 2014).

Center pivot irrigation systems apply water through several water outlets installed along a moving lateral line that rotates around a fixed point, installed at the center of a circular irrigated area (FRIZZONE et al., 2018; KELLER; BLIESNER, 1990). When compared with other irrigation systems, center pivots are flexible, easily to operable, and

present reduced labor and maintenance costs. Center pivot irrigation systems can achieve higher levels of irrigation efficiency and can be operated on terrains with variable topography (FOLEGATTI; PESSOA; PAZ, 1998). However, the cost of the equipment and its high energy demand are some of main limitations of center pivot irrigation systems.

Gilley and Watts (1977) suggested several changes in center pivot systems in order to reduce energy consumption: switching from high and medium pressure sprinklers to low pressure ones, changing nozzle size and spacing, or changing irrigation intervals and improving maintenance in order to increase pumping station efficiency. Valiantzas and Dercas (2004) developed a method to select the length of segments with different diameters from the lateral line, therefore minimizing the sum of lateral line total cost and consumed energy. Moreno et al. (2008) developed a new methodology to obtain pump characteristic curves, thereby minimizing the costs of the pumping station. In a later study, Moreno et al. (2012) stated that the energy consumption of a center pivot, which irrigates an area of 75 ha, can be minimized by adopting measures like increasing the lateral line's diameter, reducing the equipment's operating time, and increasing the flow per unit of area. While assessing the behavior of different energy efficiency indicators for a center pivot operating in an undulating topography terrain, Barbosa et al. (2018) concluded that, in order to keep adequate levels of energy used efficiency levels, center pivot machines must be continuously monitored.

Center pivot pumping stations are usually designed according to the "worst case scenario", to ensure enough water and pressure at every location in the field. The pumping unit is designed to meet the most critical situation, i.e. when the moving lateral line achieves the highest elevation point in the irrigated area, requiring the greatest pumping pressure (KING; WALL, 2000). However, due to topographic differences, pressure requirements may change as the lateral line rotates over the irrigated area. This means that the pumping station is oversized during most part of the lateral line rotation, wasting energy as excess pressure is dissipated on the pressure regulators at each outlet. One of the solutions to decrease energy waste, and consequently reducing energy consumption of irrigation systems pumping stations and/or irrigated perimeters, is the use of variable speed drives to adequate the energy supply to the actual energy system demand (FERNÁNDEZ GARCÍA et al., 2017).

Several researches have been conducted studies to verify the performance of variable speed drives in pumping stations, either for irrigated perimeters or for center pivot irrigation systems (AIT KADI et al., 1998; ALANDI et al., 2005; BRAR et al., 2017b, 2019b;

FERNÁNDEZ GARCÍA et al., 2017; HANSON; WEIGAND; ORLOFF, 1996; KING; WALL, 2000; LAMADDALENA; KHILA, 2012; MORENO et al., 2012). According to Hanson et al. (1996), the greatest potential for energy savings with variable speed drives occurs in a scenario of high electric energy rates, large horsepower reduction and long operating hours at the reduced horsepower demand. In a site where a deep-well turbine pump supplied water for several center pivots, Hanson et al. (1996) concluded that, when the pump is used to irrigate only one center pivot machine, a variable frequency drive would reduce the horsepower demand by 32%. Lamaddalena and Khila (2012) showed that 27% to 35% of energy savings can be achieved using variable speed drive in two Italian irrigation districts operating with three parallel horizontal axis pumps. In a study involving 100 standard center pivots systems installed in Nebraska (USA), Brar et al. (2017) reported that the largest potential for energy reduction (9.6%) was observed in a region with the largest elevation difference (13.6 m) between the pivot point and the highest point traversed by a pivot tower.

King and Wall (2000) stated that the optimum efficiency in terms of energy and water use can be achieved when the pumping station is able to maintain the required minimum pressure regardless of the operating conditions. Scaloppi and Allen (1993) stated that the point of minimum pressure is constantly moving along the lateral line because it is influenced by the topography of the irrigated area; they also presented theoretical bases for the calculation of this movement. However, a pumping unit working with the minimum pressure required by an irrigation system is not a guarantee of a power consumption at its minimum level, because variations in the pump operational point may cause reduction on pump efficiency, and, at lower line power frequencies, both electric motor efficiency and VFD efficiency may also suffer significant reductions (FERNÁNDEZ GARCÍA; MORENO; RODRÍGUEZ DÍAZ, 2014; MORENO et al., 2010). Therefore, reliable energy saving estimates must also consider factors that may affect variable frequency drives efficiency instead of assuming a high and constant value of VFD efficiency, (FERNÁNDEZ GARCÍA; MORENO; RODRÍGUEZ DÍAZ, 2014).

Brar et al. (2017, 2019) described the advantages, in terms of energy consumption reduction, that could be obtained when the value of total dynamic head provided by the pumping unit is automatically adjusted in order to attend changes on topographic elevations at different angular positions assumed by the lateral line during its rotation over the irrigated area. However, as reinforced by Brar et al. (2017), in order to reduce energy consumption of a

center pivot system operating with a variable speed pumping unit without compromising its water application uniformity, the pumping unit behavior, the digital elevation model of the irrigated field, and the pressure distribution along the lateral line must all be fully characterized.

The adequate description of friction head loss distribution along a center pivot lateral line has several practical applications, including VFD economic viability studies. The description of friction head loss distribution along a center pivot lateral has been receiving the attention of many researchers. Since the pioneer paper of Chu and Moe (1972) up to the publication of Tabuada (2014) proposal´s for computation of head loss distribution along center pivot lateral lines operating with and without an end gun sprinkler, several other analytical models were proposed (ALAZBA, 2005; ALAZBA et al., 2012; ANWAR, 1999, 2000; BERNUTH, 1983; REDDY; APOLAYO, 1988; SADEGHI; PETERS, 2013; TABUADA, 2011; VALIANTZAS; DERCAS, 2005). The performance of such analytical models has been assessed based on the order of magnitude of deviations of analytical estimates regarding the numeric solution of the same problem (SCALOPPI; ALLEN, 1993a; VALIANTZAS; DERCAS, 2005). However, studies assessing the relative performance of different analytical are lacking. Furthermore, the calculation process used on numerical solutions is not always adequately described, thus making harder the comparison among different analytical models described in the literature.

The EPANET hydraulic simulator (ROSSMAN, 2000) is a tool that has been used by several researchers to simulate water distribution systems (COBO et al., 2011; CÓRCOLES; TARJUELO; MORENO, 2016; FERNÁNDEZ GARCÍA et al., 2017; GARCÍA-GONZÁLEZ et al., 2015; JIMENEZ-BELLO et al., 2011; PÉREZ-SÁNCHEZ et al., 2016). Thus the EPANET hydraulic simulator (ROSSMAN, 2000) could be used as as standard tool for determining friction head loss distribution along a center pivot lateral lines.

Two articles were developed to compose the present thesis that has as general objective the study of the spatial distribution of pressure head along center pivot lateral lines operating on irrigated plots with variable topography as a tool for assessing energy reduction consumption that may be achieved with the use of a variable speed drives to adequate the energy suppled by the pumping unit to the actual energy system demand.

The first article, entitled “Pressure Distribution on Center Pivot Lateral Lines: Analytical Models Compared to EPANET 2.0”, was submitted to the *Journal of Irrigation*

and Drainage Engineering. This article covers the comparison of pressure distribution values along center pivot lateral lines, operating with and without an end gun, that were obtained by five different process including four analytical models, that were proposed by Anwar (2000), Scaloppi and Allen (1993b), Tabuada (2011) and Valiantzas and Dercas (2005), and one numerical solution, obtained through the EPANET hydraulic simulator. The main result of this study was the validation of EPANET as a center pivot lateral line analysis tool. However, the tedious process of editing EPANET input files may restrict the use of this software as center pivot hydraulic analysis tool.

The second article, entitled “Feasibility of the Use of Variable Speed Drives in Center Pivot Systems Installed in Plots with Variable Topography”, was published in the scientific journal *Water*, covers the development of a model (VSPM - Variable Speed Pivot Model). This model was developed to facilitate the process of editing EPANET input files and, furthermore, to perform the simulation of the hydraulic behavior of a center pivot system operating whit variable pumping running speed. This second article aimed to determine the feasibility of including variable speed drives in pumping stations for center pivot irrigation systems operating in variable topography plots. Considering this objective, the hydraulic simulation model of the pivot was integrated into a simulation model of the pumping station so that, with data related to topography, flow rate, and pressure, the power supply could be adjusted to the actual requirement of the system. In addition, it is useful to determine the potential of reduction from the perspective of the energy, economics, and sustainability of the installation of the variable speed drives in these irrigation systems.

2 GENERAL DISCUSSION

2.1 Concludind remarks

This research was developed to evaluate pressure distributions in different center pivot lateral line configurations through hydraulic simulations performed with the EPANET software. Pressure distribution simulations were later used in analyzing, based on reduction in energy consumption achieved, the feasibility of including a variable speed driver (VSD) in the center pivot pumping unit.

Different center pivot lateral lines configurations were hydraulically simulated with the EPANET engine. Pressure distributions obtained with EPANET were compared to pressure distributions computed with four different analytical models. Pressure distributions obtained by the different analytical processes were very similar to the ones obtained with the EPANET software, indicating that EPANET can be used as a hydraulic analysis tool for center pivot irrigation systems. A hydraulic model was also developed by aggregating topographic and energetic characteristics of a center pivot system located in Albacete (Spain). This model allowed us to verify the feasibility of including a variable speed driver (VSD) in the pumping station and the possible reduction in energy consumption of this equipment for a maize crop irrigation season.

2.2 General conclusions

Pressure distributions along center pivot lateral lines computed by using four different analytical models were very similar to the ones computed by using the EPANET hydraulic simulator. Thus, the use of EPANET as a center pivot lateral line hydraulic simulation tool was validated, however the tedious editing process of EPANET input files is a limiting factor for its use as a tool to support irrigation professionals.

For the data set of pressure distributions computed with the Darcy-Weisbach head loss equation, that considers a flow rate exponent α with an integer value equal to 2.00, the use of the more complex analytical solution (TABUADA, 2011) did not improve the relative deviation in relation to pressure values computed with the EPANET software. For the $\alpha = 2.00$ data set, all analytical solutions becoming equal to the solution proposed by Anwar (2000).

However, for the data set of pressure distributions computed using the Hazen-Williams head loss equation, that considers a flow rate exponent α with a non-integer value equal to 1.852, the analytical solution proposed by Tabuada (2011) presented a maximum relative deviation of head loss values in relation to the numerical solution computed with EPANET software of the order of 0.027%, followed by model proposed by Valiantzas and Dercas (2005) (0.106%), Scaloppi and Allen (1993) (0.933%) and Anwar (2000) (4.878%).

The VSPM -Variable Speed Pivot Model tool developed in this study was able to provide accurate estimates of energy consumption reduction that may be achieved by introducing variable frequency drives in center pivot irrigation systems that operate on an undulating terrain. For an irrigated area located in Albacete, Spain, presenting a maximum topographic elevation difference of 15.3 m, this tool was able to estimate an annual average energy savings close to 14,107.35 kWh, when using a variable instead pumping running speed of a constant pumping running speed. This reduction in energy consumption correspond to a reduction of 2,821.47 € on energy consumption expenses.

REFERENCES

AIT KADI, M. et al. Study on the possibility of energy saving in an irrigation system equipped with pumping station [Morocco]. **Irrigazione e Drenaggio**, v. 45, p. 25–30, 1998.

ALANDI, P. P. et al. Pumping Selection and Regulation for Water-Distribution Networks. **Journal of Irrigation and Drainage Engineering**, v. 131, n. 3, p. 273–281, 2005.

ALAZBA, A. A. Calculating F factor for center-pivots using simplified formula and modified Christiansen equation. **Journal of King Saud University - Science**, v. 17, n. 2, p. 85–99, 2005.

ALAZBA, A. A. et al. Field Assessment of Friction Head Loss and Friction Correction Factor Equations. **Journal of Irrigation and Drainage Engineering**, v. 138, n. 2, p. 166–176, 2012.

ALEXANDRATOS, N.; BRUINSMA, J. World agriculture towards 2030/2050: the 2012 revision. **ESA Working paper No. 12-03. Rome, FAO.**, v. 12–03, n. Query date: 2017-11-06, p. 153, 2012.

ANWAR, A. A. Friction correction factors for center-pivots. **Journal of Irrigation and Drainage Engineering**, v. 125, n. 5, p. 280–286, 1999.

ANWAR, A. A. Correction Factors for Center Pivots with End Guns. **Journal of Irrigation and Drainage Engineering**, v. 126, n. 2, p. 113–118, 2000.

AQUASTAT. FAO's global water information system. **FAO**, p. 2014, 2014.

BARBOSA, B. D. S. et al. Energy Efficiency of a Center Pivot Irrigation System. **Engenharia Agrícola**, v. 38, n. 2, p. 284–292, 2018.

BERNUTH, R. D. VON. Nozzling Considerations for Center Pivots with End Guns. **Transactions of the ASAE**, p. 419–422, 1983.

BRAR, D. et al. Energy Conservation Using Variable-Frequency Drives for Center-Pivot Irrigation: Standard Systems. **Transactions of the ASABE**, v. 60, n. 1, p. 95–106, 2017a.

BRAR, D. et al. Energy conservation using variable-frequency drives for center-pivot

irrigation: Standard systems. **Transactions of the ASABE**, v. 60, n. 1, p. 95–106, 2017b.

BRAR, D. et al. Energy Conservation using Variable Frequency Drivas for Center-Pivot Irrigation Systems Equipped with Corner Watering Attachments. v. 62, n. 5, p. 1395–1408, 2019a.

BRAR, D. et al. Energy Conservation using Variable Frequency Drives for Center Pivot Irrigations Systemas Equipped with Corner Watering Attachments. **Transactions of the ASABE**, v. 62, n. 5, p. 1395–1408, 2019b.

CHU, S. T.; MOE, D. L. Hydraulics of a Center Pivot System. **Transactions of the ASAE**, p. 894–896, 1972.

COBO, M. T. C. et al. Low energy consumption seasonal calendar for sectoring operation in pressurized irrigation networks. **Irrigation Science**, v. 29, n. 2, p. 157–169, 2011.

CÓRCOLES, J. I.; TARJUELO, J. M.; MORENO, M. A. Methodology to improve pumping station management of on-demand irrigation networks. **Biosystems Engineering**, v. 144, p. 94–104, 2016.

FERNÁNDEZ GARCÍA, I. et al. Optimal Design of Pressurized Irrigation Networks to Minimize the Operational Cost under Different Management Scenarios. **Water Resources Management**, v. 31, n. 6, p. 1995–2010, 2017.

FERNÁNDEZ GARCÍA, I.; MORENO, M. A.; RODRÍGUEZ DÍAZ, J. A. Optimum pumping station management for irrigation networks sectoring: Case of Bembezar MI (Spain). **Agricultural Water Management**, v. 144, p. 150–158, 2014.

FOLEGATTI, M. V.; PESSOA, P. C. S.; PAZ, V. P. S. Avaliação do desempenho de um Pivô Central de Grande Porte e Baixa Pressão. **Scientia Agricola**, v. 55, n. 1, p. 119–127, jan. 1998.

FRIZZONE, J. A. et al. **Irrigação por aspersão: sistema pivô central**. 1ª ed. Maringá: Editora UEM, 2018.

GARCÍA-GONZÁLEZ, J. F. et al. Use of software to model the water and energy use of an irrigation pipe network on a golf course. **Agricultural Water Management**, v. 151, p. 37–42, 2015.

GILLEY, J. R.; WATTS, D. G. Possible Energy Savings in Irrigation. **Journal of the Irrigation and Drainage Division**, v. 103, n. 4, p. 445–457, 1977.

HANSON, B. R.; WEIGAND, C.; ORLOFF, S. Variable-frequency drives for electric irrigation pumping plants save energy. **Calif Agric**, v. 50, p. 36–39, 1996.

JIMENEZ-BELLO, M. A. et al. Analysis, assessment, and improvement of fertilizer distribution in pressure irrigation systems. **Irrigation Science**, v. 29, n. 1, p. 45–53, 2011.

KELLER, J.; BLIESNER, R. D. **Sprinkle and Trickle Irrigation**. Van Nostrand Reinholh, New York: [s.n.].

KING, B. A.; WALL, R. W. Distributed Instrumentation for Optimum Control of Variable Speed Eletric Pumping Plants with Center Pivots. **Applied Engineering in Agriculture**, v. 16, n. 1, p. 45–50, 2000.

LAMADDALENA, N.; KHILA, S. Energy saving with variable speed pumps in on-demand irrigation systems. **Irrigation Science**, v. 30, n. 2, p. 157–166, 2012.

MORENO, M. A. et al. Development of a new methodology to obtain the characteristic pump curves that minimize the total cost at pumping stations. **Biosystems Engineering**, v. 102, n. 1, p. 95–105, 2008.

MORENO, M. A. et al. Energy efficiency of pressurised irrigation networks managed on-demand and under a rotation schedule. **Biosystems Engineering**, v. 107, n. 4, p. 349–363, 2010.

MORENO, M. A. et al. Optimal design of center pivot systems with water supplied from wells. **Agricultural Water Management**, v. 107, p. 112–121, 2012.

PEREIRA, L. S. Water, Agriculture and Food: Challenges and Issues. **Water Resources Management**, v. 31, n. 10, p. 2985–2999, 2017.

PÉREZ-SÁNCHEZ, M. et al. Modeling irrigation networks for the quantification of potential energy recovering: A case study. **Water (Switzerland)**, v. 8, n. 6, 2016.

REDDY, J. M.; APOLAYO, H. Friction Correction Factor For Center-Pivot Irrigation Systems. **Journal of Irrigation and Drainage Engineering**, v. 114, n. 1, p. 183–185, 1988.

ROSSMAN, L. A. EPANET 2: User Manual. **Cincinnati US Environmental Protection Agency National Risk Management Research Laboratory**, n. September, p. 104, 2000.

SADEGHI, S. H.; PETERS, T. Adjusted friction correction factors for center-pivots with an end-gun. **Irrigation Science**, v. 31, n. 3, p. 351–358, 2013.

SCALOPPI, E. J.; ALLEN, R. G. Hydraulics of Irrigation Laterals: Comparative Analysis. **Journal of Irrigation and Drainage Engineering**, v. 119, n. 1, p. 91–115, 1993a.

SCALOPPI, E. J.; ALLEN, R. G. Hydraulics of Center Pivot Laterals. **Journal of Irrigation and Drainage Engineering**, v. 119, n. 3, p. 554–567, 1993b.

TABUADA, M. A. Friction Head Loss in Center-Pivot Laterals with Single Diameter and Multidiameter. **Journal of Irrigation and Drainage Engineering**, v. 140, n. 10, p. 04014033, 2011.

TABUADA, M. A. Friction Head Loss in Center-Pivot Laterals with the Lateral Divided into Several Reaches. **Irrigation & Drainage Systems Engineering**, v. 2, n. 1, 2014.

TARJUELO, J. M. et al. Efficient water and energy use in irrigation modernization : Lessons from Spanish case studies. **Agricultural Water Management**, v. 162, p. 67–77, 2015.

VALIANTZAS, J. D.; DERCAS, N. Economic Design of Center-Pivot Sprinkler Laterals. **Journal of Irrigation and Drainage Engineering**, v. 130, n. 6, p. 491–498, 2004.

VALIANTZAS, J. D.; DERCAS, N. Hydraulic Analysis of Multidiameter Center-Pivot Sprinkler Laterals. **Journal of Irrigation and Drainage Engineering**, v. 131, n. 2, p. 137–146, 2005.

WBCSD. Water, food and energy nexus challenges. **World Business Council for Sustainable Development**, 2014.

2nd CHAPTER - ARTICLES

ARTICLE 1 - PRESSURE DISTRIBUTION ON CENTER PIVOT LATERAL LINES: ANALYTICAL MODELS COMPARED TO EPANET 2.0

Article elaborated according to standards of the *Journal of Irrigation and Drainage Engineering*, ISSN: 0733-9437 (preliminary version)

Pressure Distribution on Center Pivot Lateral Lines: Analytical Models Compared to EPANET 2.0

Victor B. S. Baptista[1]; Alberto Colombo[2]; Brenon D. S. Barbosa[3]; Lívia A. Alvarenga[4], Adriano V. Diotto[5]

[1] Professor, Agricultural Enginner, Engineering Dept., Univ. of Lavras, Campus Universitario 3037, Lavras, Brazil (corresponding author). E-mail: victor.buonosb@ufla.br

[2] Professor, Agricultural Enginner, Engineering Dept., Univ. of Lavras, Campus Universitario 3037, Lavras, Brazil. E-mail: acolombo@ufla.br

[3] Researcher, Agricultural Enginner, Posgraduate Agricultural Enginnering, Univ. of Lavras, Campus Universitario 3037, Lavras, Brazil. E-mail: b.diennevan@hotmail.com

[4] Professor, Agricultural Enginner, Engineering Dept., Univ. of Lavras, Campus Universitario 3037, Lavras, Brazil. E-mail: livia.aalvarenga@ufla.br

[5] Professor, Agricultural Enginner, Engineering Dept., Univ. of Lavras, Campus Universitario 3037, Lavras, Brazil. E-mail: adriano.diotto@ufla.br

Abstract

The analysis of friction head loss spatial distribution along center pivot lateral lines represents an important step when evaluating energy use efficiency of center pivot irrigation systems. This work compares head loss spatial distribution along center pivot lateral lines computed with the hydraulic simulator EPANET 2.0 with head loss spatial distribution predicted by four different analytical models. For the different center pivot lateral line configurations considered in this study, two different sets of values where compared: the Darcy-Weisbach equation was used for the first set, while the Hazen-Williams equation was used on the second set. On both sets, the four analytical solutions assessed in the current work estimated the head loss values similar to those computed by the hydraulic simulator EPANET 2.0. These results indicate that the detailed description of flow rate distribution along the center pivot lateral line required by the numerical method did not improve the accuracy of the head loss distribution.

On the data set of values based on Hazen-Williams equation, the analytical solution, associated with the most complex mathematical expression, provided the lowest deviation in relation to head loss values computed by EPANET 2.0. On the data set of values based on the Darcy-Weisbach, assuming a fully turbulent flow regime, the four analytical models presented the same deviation in relation to the values computed by EPANET 2.0.

Keywords: Center pivot irrigation; Pressure distribution; Head loss correction factor; End gun sprinkler.

Introduction

The adequate knowledge on the spatial distribution of head loss along the length of center pivot lateral lines has increased practical applications for development of strategies to reduce the energy consumption in these irrigation systems. Based on the spatial distribution pattern of head loss along center pivot lateral lines, Valiantzas and Dercas (2004) developed a method to select the length of segments with different diameters from the lateral line, therefore minimizing the sum of the line total cost and consumed energy. Brar et al. (2017, 2019) described the advantages, in terms of energy consumption reduction, that could be attained when the value of total dynamic head provided by the pumping unit is automatically adjusted to attend topographic variation of different angular positions assumed by the lateral lines during its rotation on the irrigated area. Such adjustment avoids that the maximum value of total dynamic head (that meet the greatest condition of topographic difference along the entire rotation of lateral line) is applied at lower topographic differences. However, as reinforced by Brar et al. (2017), in order to reduce energy consumption of a center pivot system operating with a variable speed pumping unit without compromising its water

application uniformity, the pumping unit operation, the digital elevation model of the irrigated field, and the pressure distribution along the lateral line must all be fully characterized.

Due to several practical applications that require a detailed description of the head loss distribution along the length of a center pivot lateral, this topic has received the attention of several researches. Since the publication of the pioneer work of Chu and Moe (1972) until the most recent proposal of Tabuada (2014), several alternatives were published on the analytical calculation of friction head loss distribution along center pivot lateral lines. The performance of such analytical models has been assessed based on the order of magnitude of deviations of estimates regarding the numeric solution of the same problem (Scaloppi and Allen 1993a; Valiantzas and Dercas 2005). However, studies comparing the relative performance of different analytical with the results of the same numerical solution models are lacking. Furthermore, the calculation process used on numerical solutions is not always adequately described, thus making harder the comparison among different analytical models described in the literature.

The present work aimed to compare the performance of four different analytical models that have been used to calculate the spatial distribution of the head loss along center pivot lateral line. The performance of Scaloppi and Allen (1993a), Anwar (2000), Valiantzas and Dercas (2005) and Tabuada (2011) models were compared in this study. These models were developed from the same basic hypothesis of continuous discharge of water along an irrigation lateral line of radial displacement, however they result in mathematical expressions with different levels of complexity. The Anwar (2000) model is associated to the simplest mathematical expression among the four evaluated models, while the solution proposed by Tabuada (2011) requires the evaluation of the hypergeometric function for different values assumed by its arguments.

In the present work, the numerical solutions used in assessing the performance of different analytical models were obtained by hydraulic simulations carried out with the software EPANET 2.0 (Rossman 2000). The use of such software ensures the quality of the numerical solutions, since the quality of hydraulic simulations of EPANET 2.0 has been extensively validated by several studies (Córcoles et al. 2016; Fernández García et al. 2017; García-González et al. 2015; Moreno et al. 2008). Moreover, since EPANET 2.0 has an open source and is freely distributed, the detailed description of EPANET´s input files that were developed for this study will allow other researchers the opportunity to reproduce the same numerical results presented along this paper.

Material and Methods

Validation of EPANET 2.0 numerical solutions

Considering that all numerical solutions were carried on with the hydraulic simulator EPANET 2.0 (Rossman 2000), the first step of the present work involved the assessment of the procedure used for creating EPANET 2.0 input files. The assessment process was based on the19 values of total head loss along center pivot lateral lines that are shown in Table 1. These values were reported by Valiantzas and Dercas (2005). A standard numerical method (stepwise method) was used to determine these head loss values. All 19 lateral lines configurations shown in Table 1 are 402 m long (L_T) and present 134 outlets at uniform 3 m spacing. The first eighteen of such configurations considered a center pivot lateral operating without an end gun sprinkler. These first eighteen configurations were obtained by combining three different inner pipe diameter options, three different values of pipe wall absolute roughness (ε = 0.03 mm, ε = 0.10 mm and ε = 0.40 mm) and two different gross irrigation depth values (d_G = 5 mm and d_G = 12 mm) applied in a 24 h center pivot lateral line revolution time. As indicated in Table 1, the following three pipe diameter options were considered: (i) a 402 m long lateral line with a 0.168 m pipe diameter; (ii) a 402 m long lateral line with a 0.127 m pipe diameter, and (iii) a 402 m long lateral composed by a 201m long upstream section with the largest piper diameter (0.168 m) and a 201m long downstream section with the smaller pipe diameter (0.127 m). For the nineteenth configuration presented in Table 1, an end gun sprinkler with a 22.716 m^3 h^{-1} discharge was considered in the 402 m long lateral, presenting a 252 m long upstream segment with a 0.168 m pipe diameter and a 150 m long downstream segment with a 0.127 m pipe diameter. For this nineteenth configuration, the pipe wall absolute roughness value was set as ε = 0.15 mm and the outlets

flow rate values were computed based on a 8 mm gross irrigation depth applied within a 24 h center pivot rotation time.

Table 1. Configurations of the center pivot lateral line, numerical estimates of head loss ($hf_{x=L_T}$) of Valiantzas and Dercas (2005) and EPANET 2.0, with the respective deviations in relation to EPANET 2.0.

Lateral characteristics[a] (L_T = 402 m)					ε	gr	Numerical solutions (α = 2.0)		
N°	L_U	D_U	D_D	d_G			$hf^{N}_{x=L_T}$ [a]	$hf^{EPA}_{x=L_T}$	Error[b]
	m	mm	mm	mm/24h	mm		m	m	%
1	402	168	-	5	0.03	0.00	1.968	1.970	-0.102
2	201	168	127	5	0.03	0.00	3.250	3.253	-0.092
3	402	127	-	5	0.03	0.00	7.876	7.882	-0.076
4	402	168	-	12	0.03	0.00	10.214	10.220	-0.059
5	201	168	127	12	0.03	0.00	16.953	16.962	-0.053
6	402	127	-	12	0.03	0.00	41.811	41.828	-0.041
7	402	168	-	5	0.10	0.00	2.239	2.240	-0.045
8	201	168	127	5	0.10	0.00	3.738	3.739	-0.027
9	402	127	-	5	0.10	0.00	9.295	9.298	-0.032
10	402	168	-	12	0.10	0.00	12.160	12.164	-0.033
11	201	168	127	12	0.10	0.00	20.394	20.399	-0.025
12	402	127	-	12	0.10	0.00	51.403	51.412	-0.018
13	402	168	-	5	0.40	0.00	2.926	2.927	-0.034
14	201	168	127	5	0.40	0.00	4.949	4.950	-0.020
15	402	127	-	5	0.40	0.00	12.607	12.609	-0.016
16	402	168	-	12	0.40	0.00	16.478	16.479	-0.006
17	201	168	127	12	0.40	0.00	27.936	27.939	-0.011
18	402	127	-	12	0.40	0.00	71.580	71.585	-0.007
19	252	168	127	8	0.15	0.118	11.420	11.424	-0.035

[a] pivots 1 to 18: numerical solutions as extracted from Table 1 of Valiantzas and Dercas (2005); pivot 19 of the application example of Valiantzas and Dercas (2005); [b] relative to EPANET 2.0.

EPANET 2.0 Input files

As illustrated in Fig. 1, the 402 m long lateral line with 134 outlets at uniform 3 m spacing was represented in the EPANET 2.0 input files as a branched hydraulic network containing 135 Junctions and 134 Links (pipes).

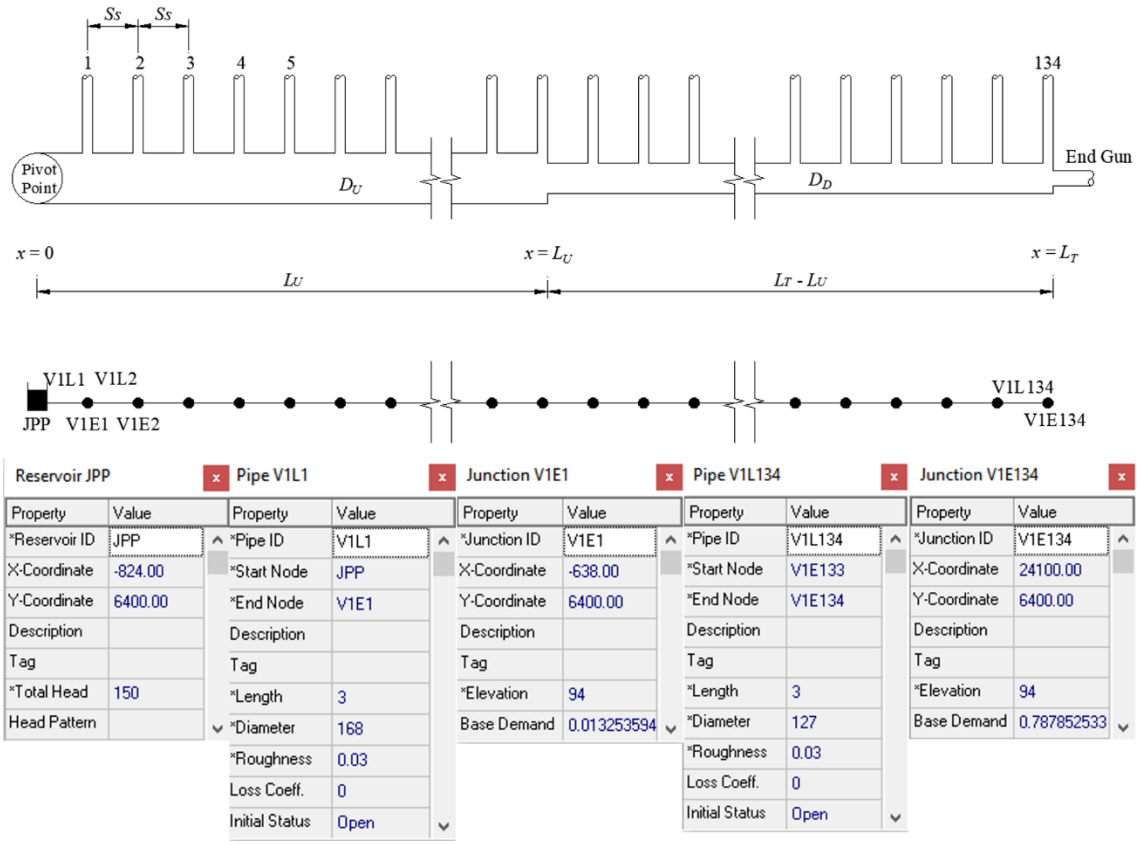

Fig. 1. Main properties of junctions and pipes of the representation in EPANET 2.0 of a center pivot lateral line with 134 outlets equally spaced at each 3.0 m (L_T = 402 m; L_U = 201 m; D_U = 168 mm; ε = 0.03 mm; D_D = 127 mm, d_G = 5 mm; T_c = 24 h).

In order to accelerate the editing process of properties of the 269 elements of this network, the EPANET 2.0 input files were edited in Excel spreadsheets that were saved as text files with extension INP (Rossman 2000). In the EPANET 2.0 hydraulic network representation of the center pivot literal line, a reservoir-type junction (*Reservoir* JPP, Fig. 1), with a total head value set as 150 m, was to represent the center pivot lateral line inlet at the top of the pivot point pipe. On EPANET 2.0 graphic display, the position of the point representing the center pivot lateral inlet was determined by the coordinates X = -824 and Y =

6 400. Such coordinates correspond to a point randomly chosen in the upper left corner of the EPANET 2.0 graphic display. The junctions representing the lateral line outlets were identified by a name resultant from the acronym "V1E" jointed with the lateral line outlet order number "*i*" ($1 \leq i \leq 134$). The value of the graphic coordinate *Y* of these junctions remained equal to those used at the inlet of the center pivot lateral line (*Y*= 6400). The value of the graphic coordinate *X* of successive water outlets was determined based on a constant increase of 186 units from the value of coordinate X of the junction JPP: $X = -824 + i\,(186)$. A constant value equal to 94 m was attributed to the geometric elevation (*Elevation*, Fig. 1) of all junctions representing water outlets. The flow rate value of each outlet ($m^3\ h^{-1}$) was set in the parameter *base demand* .Outlet flow rate values were computed according to the procedure used by Valiantzas and Dercas (2005), as described by Eqs. (1) to (3):

$$q_{i=1} = \frac{\pi\left(Ss + \frac{Ss}{2}\right)^2}{1000}\frac{d_G}{T_c}\ \text{, for } i=1 \tag{1}$$

$$q_i = \frac{2\pi Ss^2 i}{1000}\frac{d_G}{T_c}\text{, for } 2 \leq i \leq 133 \tag{2}$$

$$q_{i=134} = \frac{\pi Ss^2\left(i - \frac{1}{4}\right)}{1000}\frac{d_G}{T_c}\text{, for } i=134 \tag{3}$$

where:

q_i – flow rate (*base demand in EPANET 2.0*) of outlet i ($1 \leq i \leq 134$), $m^3\ h^{-1}$;

Ss – uniform outlet spacing, m;

d_G – gross irrigation depth applied within the time period required for a complete lateral line revolution, mm;

T_c – time period required for a complete lateral line revolution;

1000 – factor corresponding to 1000 mm m^{-1}.

For the nineteenth configuration presented in Table 1, the flow rate value of the last emitter (q_{134}) was assumed equal to end gun sprinkler flow rate (22.716 $m^3 h^{-1}$), resulting on a flow rate value equal to 191.95 $m^3 h^{-1}$ at the center pivot inlet, that correspond to a 0.118 end-gun ratio value.

In the EPANET 2.0 input files, each one of the 134 pipes required to link the 135 junctions of the hydraulic network was identified by a name corresponding to the acronym "V1L" added to the order number "*i*" of the junction downstream each segment (V1L1, V1L2, ... and V1L134, Fig. 1). In these files, besides the identification of pipes, it was also necessary to specify: (i) the start node and end node of each pipe; (ii) the length of each pipe, which was assumed to be constant and equal to the spacing between outlets (*Ss* = 3.0 m); (iii) the pipe inner diameter, in mm; and (iv) pipe wall roughness. In the cases of Hazen-Williams and Darcy-Weisbach equations, the information inserted in the field regarding the pipe wall roughness corresponded, respectively, to the dimensionless coefficient characteristic of the pipe material (C_{HW} coefficient) and to the value of pipe wall absolute roughness, in mm.

Numerical calculation of the head loss distribution

The head loss spatial distribution along center the pivot lateral line was determined based on values of the total hydraulic head available on each one of the 134 outlets of the lateral line that were taken from EPANET 2.0 output files. The head loss from the lateral line inlet up to each one of the 134 outlets was compute in a separated spreadsheet. In this spreadsheet differences among total head value at the of lateral inlet (junction JPP, Fig. 1), that was assumed equal to 150 m, and the total head value at each outlet, as specified at EPANET 2.0 output files, were computed. In this sense, the value of head loss along the

entire physical length of each center pivot lateral line composition was obtained by the difference between the of total hydraulic head value at the junction JPP (150 m) and the total hydraulic head value at the last lateral junction (junction V1E134, Fig. 1).

Analytical calculation of the head loss distribution

Analytical calculation of the head loss distribution along a center pivot lateral line may be derived assuming that the outflow varies continuously in space along the center-pivot lateral line. The total flow rate Q_x at any point along a lateral line section at distance x from the lateral inlet, can be calculated as:

$$Q_x = Q_0\left[1-\left(\frac{x}{L_{Eq}}\right)^2\right] \qquad \text{for } 0 \le x \le L_T \tag{4}$$

where

Q_0 – total flow rate at the inlet of the center pivot lateral with a value that corresponds to the sum of the discharge rate of all center pivot outlets, including the end gun discharge rate;

Q_x – flow rate at point x;

x – distance taken from the lateral line inlet at the pivot point;

L_{Eq} – the equivalent hydraulic length of a center pivot lateral line.

The equivalent hydraulic length is computed based on the physical length of the center pivot lateral line and the ratio of end gun flow rate and the center pivot inlet flow rate (Q_0):

$$L_{Eq} = \frac{L_T}{\sqrt{1-gr}} \tag{5}$$

L_T – physical length of the center pivot lateral line;

gr – end gun ratio, the ratio of end gun flow rate and the center pivot inlet flow.

Valiantzas and Dercas (2005) have demonstrated that for a single diameter center pivot lateral line, the pipe friction head loss between the center pivot lateral line inlet hf_x (in the radial distance x ($0 \le x \le L_T$)) can be estimated as:

$$hf_x = Sf_{D_U} \int_0^x \left[1 - \left(\frac{s}{L_{Eq}} \right)^2 \right]^\alpha ds \qquad \text{for } 0 \le x \le L_T \tag{6}$$

Sf_{D_U} – head loss per unit length of a pipe with inner diameter D_U conducting the center pivot lateral line inlet discharge Q_0;

α – flow rate exponent in the head loss equation used to compute Sf_{D_U} .

Anwar (2000), Valiantzas and Dercas (2005) and Tabuada (2011) developed correction factors for the spatial head loss distribution along center pivot lateral lines with an end gun based on the total head loss that would be observed on a similar fictitious pipe with single diameter D_U, conducting a constant flow Q_0 over the entire physical length of the center pivot lateral line ($Sf_{D_U} L_T$):

$$hf_x = \left(Sf_{D_U} L_T \right) \left\{ \frac{1}{L_T} \int_0^x \left[1 - \left(\frac{s}{L_{Eq}} \right)^2 \right]^\alpha ds \right\} \qquad \text{for } 0 \le x \le L_T \tag{7}$$

Considering that the second term in Eq. (7) is a correction factor for the spatial head loss distribution along a center pivot lateral line, and after introducing an λ index for identification of friction correction values (F_x^λ) and head loss values (hf_x^λ) associated to each one of the four analytical models considered in this study(λ = "S" for Scaloppi and Allen (1993); λ = "A" for Anwar (2000); λ = "V" for Valiantzas and Dercas (2005) and λ = "T" for Tabuada (2011)), Eq. (7) may be expressed as:

$$hf_x^\lambda = \left(Sf_{D_U} L_T\right) F_x^\lambda \qquad \text{for } 0 \le x \le L_T \tag{8}$$

where:

hf_x^λ – pipe friction head loss between the center pivot lateral line inlet and the radial distance *x* estimated with the analytical model identified by the λ index;

F_x^λ – center pivot head loss distribution correction factor for the radial distance *x*.

For all analytical models assed in this study center pivot head loss distribution correction factor was computed as:

$$\mathrm{F}_x^\lambda = \frac{1}{L_T}\int_0^x \left[1-\left(\frac{s}{L_{Eq}}\right)^2\right]^\alpha ds \qquad \text{for } 0 \le x \le L_T \tag{9}$$

Chu and Moe (1972) pointed out that, when the flow exponent α assumes a non-integer value (ie. α =1.9), there is no trivial solution for the integral in Eq. (7) and (9). These authors also developed a "trivial" solution for the integral in Eq. (7) and (9) considering the particular case in which the flow exponent α is set as equal to 2.0(Chu and Moe 1972).

Scaloppi and Allen (1993b) presented a trivial solution for α =1.0 for center pivot lateral lines operating with an end gun, Anwar (2000) developed a head loss distribution correction factor based on the trivial solution that assumes α = 2.0. For this reason, along this paper, the analytical solution based on a constant value of α = 2.0 in Eq. (7) and (9) is referred as the "Anwar (2000) solution". The correction head loss distribution correction factor based on the trivial solution that assumes α = 2.0 is given by:

$$F_x^{\lambda=A} = \left[\frac{x}{L_T} - \frac{2}{3}(1\text{-}gr)\left(\frac{x}{L_T}\right)^3 + \frac{1}{5}(1\text{-}gr)^2\left(\frac{x}{L_T}\right)^5 \right] \tag{10}$$

Scaloppi and Allen (1993a) proposed the use of truncated expansion of a binomial approximation to $(1\text{-}(s/L_{Eq})^2)^{\alpha}$ in Eq. (9). After inserting the truncated approximation used by Scaloppi and Allen (1993a), the head loss distribution correction factor indicated in Eq. (9) becomes:

$$F_x^{\lambda=S} = \left[\frac{x}{L_T} - \frac{\alpha}{3}(1-gr)\left(\frac{x}{L_T}\right)^3 + \frac{\alpha(\alpha-1)}{10}(1-gr)^2\left(\frac{x}{L_T}\right)^5 - \frac{\alpha(\alpha-1)(\alpha-2)}{42}(1-gr)^3\left(\frac{x}{L_T}\right)^7 \right] \tag{11}$$

Valiantzas and Dercas (2005) developed a "more compact" expression that, in the range of $1.75 \leq \alpha \leq 2.0$ and $0 \leq gr \leq 1$, provides an approximation for the truncated binomial expansion used by Scaloppi and Allen (1993a) to replace $(1\text{-}(s/L_{Eq})^2)^{\alpha}$. After inserting in Eq. (9) the approximation to $(1\text{-}(s/L_{Eq})^2)^{\alpha}$ proposed by Valiantzas and Dercas (2005), the head loss distribution correction factor indicated in Eq. (9) becomes:

$$F_x^{\lambda=V} = \left[\frac{x}{L_T} - \frac{\alpha}{3}(1-gr)\left(\frac{x}{L_T}\right)^3 + \frac{(\alpha-1)}{7-\alpha}(1-gr)^{3-\frac{\alpha}{2}}\left(\frac{x}{L_T}\right)^{7-\alpha} \right] \quad (12)$$

Scaloppi and Allen (1993b), for the case of a center pivot lateral line operating without an end gun, and Tabuada (2011), also for the case of a center pivot lateral line operating without an end gun, pointed out that by changing the integration variable in Eq. (9), from θ equal to (1-(s/L_{Eq})^2), the correction factor in Eq. (9) could be computed with the help of the incomplete beta function:

$$F_x^{\lambda=T} = \frac{1}{2\sqrt{1-gr}} \int_0^{\left(x/L_T\right)^2 (1-gr)} \theta^{1/2-1}(1-\theta)^{(\alpha+1)-1}\, d\theta = \frac{B_{in}\left[\left(\frac{x}{L_T}\right)^2 (1-gr); \frac{1}{2}; \alpha+1\right]}{2\sqrt{1-gr}} \quad (13)$$

where:

B_{in} – incomplete beta function;

θ – integration variable equal to (s/L_{Eq})^2.

By applying the hypergeometric function representation of the incomplete beta function showed in Eq. (13), Tabuada (2011) proposed the following expression to Eq. (13):

$$F_x^{\lambda=T} = \left(\frac{x}{L_T}\right) F_{hyper}\left[0.5; -\alpha; 1.5; (1-gr)\left(\frac{x}{L_T}\right)^2\right] \quad (14)$$

For the analytical model proposed by Tabuada (Eq. (9)), values of the hypergeometric function (F_{hyper} [ ]) were computed with an Excel® spreadsheet. An Excel Visual Basic for Applications – VBA macro was implemented based on an adaptation of the calculation process described by Chandrupatla and Osler (2010), as demonstrated in Fig. 2.

```
Function hgs(a, b, c, z)
t = a * b / c * z
s = 1 + t
n = 1
Do
  a = a + 1: b = b + 1: c = c + 1: n = n + 1
  t = t * a / c * b / n * z
  s1 = s
  s = s + t
  If s <> 0 Then Delta = Abs(s - s1) / s
  If s = 0 Then Delta = Abs(s - s1)
Loop While Delta > 0.00001
hgs = s
End Function
```

Fig. 2. VBA routine for the hypergeometric function (F_{hyper} [ ]) calculation.

Center pivot correction factors showed on Eq. (10) to (14) may also be applied for computing the head loss distribution along a center pivot lateral line presenting reaches with two different pipe diameters. Considering , as indicated in Fig.1, that the dual diameter lateral line has an upstream reach, with a length equal to L_U and inner pipe diameter D_U, and downstream reach, with length equal to $(L_T - L_U)$ and inner pipe diameter D_D, all head loss values, accumulated from the center pivot lateral line inlet (x = 0 m) up to any point located along the physical length of the lateral line (0 m $\leq x \leq L_T$), may be computed according to two possibilities, as described by Allen et al (2011):

for $0 \le x \le L_U$

$$hfd_x = Sf_{D_U} L_T \left\{ \frac{1}{L_T} \int_0^x \left[1 - \left(\frac{s}{L_{Eq}} \right)^2 \right]^\alpha ds \right\} \tag{15}$$

for $L_U < x \le L_T$

$$\begin{aligned} hfd_x = {} & Sf_{D_U} L_T \left\{ \frac{1}{L_T} \int_0^{L_U} \left[1 - \left(\frac{s}{L_{Eq}} \right)^2 \right]^\alpha \right\} ds + \ldots \\ & Sf_{D_D} L_T \left\{ \left\{ \frac{1}{L_T} \int_0^x \left[1 - \left(\frac{s}{L_{Eq}} \right)^2 \right]^\alpha ds \right\} - \left\{ \frac{1}{L_T} \int_0^{L_U} \left[1 - \left(\frac{s}{L_{Eq}} \right)^2 \right]^\alpha ds \right\} \right\} \end{aligned} \tag{16}$$

where:

hfd_x – pipe friction head loss for dual-diameter between the center pivot lateral line inlet and the radial distance x;

Sf_{D_D} – head loss per unit length of a pipe with inner diameter D_D conducting the center pivot lateral line inlet discharge Q_0;

L_U – upstream lateral line length.

By inserting in Eq. (15) and (16) the correction factors corresponding to the analytical model to be assessed (λ = “S” for Scaloppi and Allen (1993a); λ = “A” for Anwar (2000); λ = “V” for Valiantzas and Dercas (2005) and λ = “T” for Tabuada (2011)) the head loss values for a dual-diameter center pivot lateral line are computed by:

for $0 \le x \le L_U$ then $hfd_x^\lambda = \left(Sf_{D_U} L_T \right) F_x^\lambda$, (17)

for $L_1 < x \leq L_T$ then $$hfd_x^{\lambda} = \left(Sf_{D_U} L_T\right) F_{L_U}^{\lambda} + \left(Sf_{D_D} L_t\right)\left(F_x^{\lambda} - F_{L_U}^{\lambda}\right), \quad (18)$$

where:

$F_{L_U}^{\lambda}$ – center pivot head loss distribution correction factor for the radial distance L_U.

When the rate of head loss per unit length (Sf_D) was calculated with the Darcy-Weisbach equation, the friction factor was determined with the Swamee and Jain equation (Swamee and Jain 1976), following the same procedure used by both Valiantzas and Dercas (2005) and EPANET 2.0 (Rossman 2000). In this case, according to the same procedure adopted by Valiantzas and Dercas (2005) and Tabuada (2011, 2014), the flow rate exponent value considered was the one corresponding to the fully turbulent regime ($\alpha = 2.0$):

$$Sf_D = \frac{8f}{\pi^2 g} \frac{Q_0^{\,2}}{D^5} \quad (19)$$

where:

D – center pivot lateral line inner diameter (D_U or D_D);

f – friction coefficient of the Darcy–Weisbach equation;

g – gravitational acceleration, m s^{-2}.

When the head loss rate (Sf_D) was calculated with the Hazen-Williams equation, the same values of empirical coefficients described in the EPANET 2.0 manual (Rossman 2000) were considered: flow rate exponent $\alpha = 1.852$; pipe diameter exponent of -4.871 and a conversion constant for metric units of 10.667 $s^{1.852}$ $m^{-0.685}$, which corresponds to 4.727 $s^{1.852}$ $ft^{-0.685}$.

$$Sf_D = \frac{10.667}{D^{4.871}} \left(\frac{Q_o}{C_{HW}} \right)^{1.852} \quad (20)$$

where:

C_{HW} – friction coefficient for the Hazen–Williams equation

Analytical calculation of pressure head distribution

Pressure head spatial distributions along a center pivot lateral were computed for the different four analytical models considered (λ = S, A, V, or T) considering the nineteenth configuration presented in Table 1, under two different ground slope values (S_0 = 0 and S_0 = -0.02). For pressure head spatial distributions based on the Darcy-Weisbach head loss an absolute roughness ε = 0.15mm was considered. For pressure head spatial distributions based on the Hazen-Williams head loss equation roughness coefficient C_{HW} = 135 was used.

The pressure head value at any outlet located along the center pivot lateral line physical length (0 m < $x \leq L_t$) was computed according to Eq. (21):

$$h_x^{\lambda} = h_0 - \left(S_0 x \right) - hf_x^{\lambda} \quad (21)$$

where

h_x^{λ} – pressure head at radial distance x (0 m ≤ $x \leq L_T$) from the pivot point estimated by the analytical model identified by the λ index, m;

h_0 – pressure head at the pivot point, m;

S_0 – constant slope of the ground elevation, m m^{-1} ($S_0 > 0$ uphill, $S_0 < 0$ downhill).

Results and Discussion

Validation of the procedure for data input in EPANET 2.0

Comparison among total head loss values along center pivot lateral lines, obtained by Valiantzas and Dercas (2005), with the standard numerical calculation process (stepwise method) and total head loss values along the same center pivot lateral lines estimated with EPANET 2.0 hydraulic simulator, are presented on Table 1. The small deviations (< 0.102%) in relation to EPANET 2.0 that are presented in Table 1, confirm the adequacy of the procedure used in the present study to generate EPANET 2.0 input files representing the 19 different configurations considered by those authors.

The differences between head loss values presented in Table 1, which are in the order of millimeters of water head, do not have any practical effect. However, these small differences reinforce the advantage of using EPANET 2.0, allow other researchers to reproduce exactly the same numerical results as presented in this study, when using the same process described here for writing EPANET 2.0 input files. Besides this, is important to point out that the process required for editing EPANET 2.0 input file is very time-consuming. In this study a spreadsheet was used in order to set base demand values and elevation values for the 135 junctions representing the center pivot lateral line inlet ant its 134 outlets.

Analytical methods with Darcy-Weisbach equation

When Darcy-Weisbach equation is used, the flow rate exponent depends on the flow regime considered (Valiantzas 2005): α = 1.0 for the laminar flow; α = 1.75 for smooth turbulent regime; and α = 2.0 for the completely turbulent regime (Scaloppi and Allen 1993a).

For the particular case of α = 2.0, which was the particular α value considered in the present study when considering the Darcy-Weisbach head loss equation, it is easy to demonstrate, that, when α = 2.0, the analytical solutions of Scaloppi and Allen (1993a) and Valiantzas and Dercas (2005), described respectively by Eq. (11) and (12), assume the same mathematical representation of Eq. (10), that was proposed to Anwar (2000). It is not so easy, by simply examining Eqs. (14) and (10), that for the particular case of α = 2.0, F_x values computed with the hypergeometric function (Fhyper [ ] of Eq. (14)), as recommended by Tabuada (2011, 2014), are exactly the same as the ones given by Eq. (10). The equivalence between Eqs. (14) and (10), when α = 2.0, was demonstrated by Tabuada (2011), that pointed out that, due to its complexity, use of Eq. (14) should be limited to non-integer real values of α.

The equivalence, for the particular case of α = 2.0, between Eq. (14) and the other analytical models (Eqs. (10), (11) and (12)) is demonstrated in Table 2, considering the first six of the nineteen center pivot lateral lines configurations presented in Table 1. In order to demonstrate that the equivalence observed among the four assessed analytical solutions also includes center pivot lateral lines with end gun sprinkler ($gr > 0$), the results of two additional simulations were included in Table 2 considering, for the second lateral line configuration described in Table 1, flow rate values of 10 and 20% for the total lateral line flow rate, resulting on gun ratio values of, respectively gr = 0.1 and gr = 0.2.

Table 2. Configurations of lateral lines, values of head loss of EPANET 2.0 and analytical solutions of Anwar and Tabuada, with the respective deviations in relation to EPANET 2.0 when the Darcy-Weisbach equation is used.

Lateral characteristics			EPANET 2.0	Analytical solutions (α = 2.0)			
Nº	ε	gr	$hf_{x=L_T}^{EPA}$	$hf_{x=L_T}^{A}$	Error[a]	$hf_{x=L_T}^{T}$	Error[a]
	mm		m	m	%	m	%
1	0.03	0.00	1.970	1.915	-2.792	1.915	-2.792
2	0.03	0.00	3.253	3.113	-4.304	3.113	-4.304
2	0.03	0.10	4.387	4.211	-4.012	4.211	-4.012
2	0.03	0.20	6.036	5.859	-2.932	5.859	-2.932
3	0.03	0.00	7.882	7.703	-2.271	7.703	-2.271
4	0.03	0.00	10.220	10.023	-1.928	10.023	-1.928
5	0.03	0.00	16.962	16.484	-2.818	16.484	-2.818
6	0.03	0.00	41.828	41.229	-1.432	41.229	-1.432

[EPA] EPANET 2.0; [A] Anwar (2000); [T] Tabuada (2011, 2014); [a]relative to EPANET 2.0.

The equivalence among the four analytical methods (Eqs. (10), (11), (12) and (14)) demonstrated in the present study indicates that when Darcy-Weisbach equation (α = 2.0, is used) the solution of Anwar (2000), as described by Eq. (10), must be used, since the complexity of the other analytical models does not improve the accuracy of the obtained results.

Finally, it is also interesting to observe in Table 2 that when Darcy-Weisbach equation is considered, analytical solutions provided values of total head loss along center pivot lateral lines always lower than those obtained by the numerical method ($hf_{x=L_T}^{Analytical} - hf_{x=L_T}^{EPA} < 0$). Valiantzas and Dercas (2005) had already observed that, when Darcy-Weisbach equation is used in computing head loss along center pivot lateral lines. The authors justified such behavior based on the fact that when such equation is used, the analytical method is not affected by the small increase in the friction factor caused by the reduction of Reynolds number along the lateral line, which is considered by the numerical method. Tabuada (2011, 2014) justified this same behavior based on the type of flow rate variation along the lateral

line considered by each method. According to this author, analytical methods based on the continuous variation of flow rate along the lateral line result in a lower head loss than the numerical method, which considers a discrete variation of flow rate along the lateral line. Sadeghi and Peters (2013) also observed that estimates of head loss in center pivot lateral line regarding analytical methods, which are based on continuous variations of flow rate, are lower than estimates of head loss obtained by the numerical process. These authors highlight that such differences tend to increase when the number of outlets in the lateral line is reduced. Sadeghi and Peters (2013) demonstrated such behavior citing an example in which the deviation between the analytical solution of Valiantzas and Dercas (2005) in relation to the numerical method passes from -1% to -4% when outlets considered in the center pivot lateral line is reduced from 134 to 20.

Analytical methods using Hazen-Williams equation

When Hazen-Williams equation is considered to calculate the head loss, the flow rate exponent assumes a constant value (Valiantzas 2005) equal to 1.852 (α=1.852). In this condition, as demonstrated in Tables 3 and 4, the estimates of total head loss provided by the four analytical solutions (Eqs. (10), (11), (12) and (14)) are not the same.

Table 3. Configurations of lateral lines values of head loss in EPANET 2.0 and of analytical solutions of Scaloppi and Anwar with the respective deviations in relation to EPANET 2.0 when the Hazen-Williams equation is used.

Lateral characteristics			EPANET 2.0	Analytical solutions (α = 1.852)			
Nº	C_{HW}	gr	$hf^{EPA}_{x=L_T}$	$hf^{S}_{x=L_T}$	Error[a]	$hf^{A}_{x=L_T}$	Error[a]
			m	m	%	m	%
1	135	0.0	2.302	2.293	-0.391	2.240	-2.693
2	135	0.0	3.772	3.737	-0.928	3.588	-4.878
2	135	0.1	5.070	5.045	-0.493	4.827	-4.793
2	135	0.2	7.002	6.983	-0.271	6.680	-4.599
3	135	0.0	8.995	8.960	-0.389	8.752	-2.702
4	135	0.0	11.650	11.604	-0.395	11.335	-2.704
5	135	0.0	19.085	18.907	-0.933	18.156	-4.868
6	135	0.0	45.516	45.338	-0.391	44.285	-2.705

[S] Scaloppi and Allen (1993a); [A] Anwar (2000); [a] relative to EPANET 2.0.

Table 4. Configurations of lateral lines, values of head loss of EPANET 2.0 and analytical solutions of Valiantzas and Tabuada, with the respective deviations in relation to EPANET 2.0 when the Hazen-Williams equation is used.

Lateral characteristics			EPANET 2.0	Analytical solutions (α=1.852)			
Nº	C_{HW}	gr	$hf^{EPA}_{x=L_T}$	$hf^{V}_{x=L_T}$	Error[a]	$hf^{T}_{x=L_T}$	Error[a]
			m	m	%	m	%
1	135	0.0	2.302	2.302	0.000	2.302	0.000
2	135	0.0	3.772	3.776	0.106	3.771	-0.027
2	135	0.1	5.070	5.072	0.039	5.070	0.000
2	135	0.2	7.002	6.997	-0.071	7.002	0.000
3	135	0.0	8.995	8.995	0.000	8.995	0.000
4	135	0.0	11.650	11.650	0.000	11.649	-0.009
5	135	0.0	19.085	19.105	0.105	19.084	-0.005
6	135	0.0	45.516	45.517	0.002	45.515	-0.002

[V] Valiantzas and Dercas (2005); [T] Tabuada (2011, 2014); [a] relative to EPANET 2.0.

The column corresponding to the analytical solution of Anwar (2000) in Table 3 presents the highest absolute values of deviations in relation to EPANET 2.0 regarding the use of Hazen-Williams equation. Such behavior is justified, since for the case of Hazen-Williams

equation, the analytical solution of Anwar (2000) results from rounding the flow rate exponent of α= 1.852 to α= 2.0. Except for the analytical solution of Anwar (2000), the other solutions at Table 3 and 4 presented lower absolute values in relation to EPANET 2.0 than those presented on Table 2. Such improvement of performance of analytical solutions of Scaloppi and Allen (1993a), Valiantzas and Dercas (2005) and Tabuada (2011) in relation to the numerical method is expected when the Darcy-Weisbach equation is replaced by the Hazen-Williams one. For the case of the Hazen-Williams equation, both analytical (Scaloppi and Allen 1993a; Tabuada 2011; Valiantzas and Dercas 2005) and numerical methods assume the same constant friction coefficient value (C_{HW}) along the lateral line length.

When comparing the values presented by Table 3 and 4, it is possible to conclude that the solution of Tabuada (2011) is superior to the Valiantzas and Dercas (2005), which is superior to the solution of Scaloppi and Allen (1993a). However, the superior performance of the solution of Valiantzas and Dercas (2005) in relation to Scaloppi and Allen (1993a) only is observed when comparing values of accumulated head loss related to the overhang of the lateral line. This behavior is better demonstrated when the deviations in relation to EPANET 2.0 are computed for different distances from the center pivot, as demonstrated in Fig. 3.

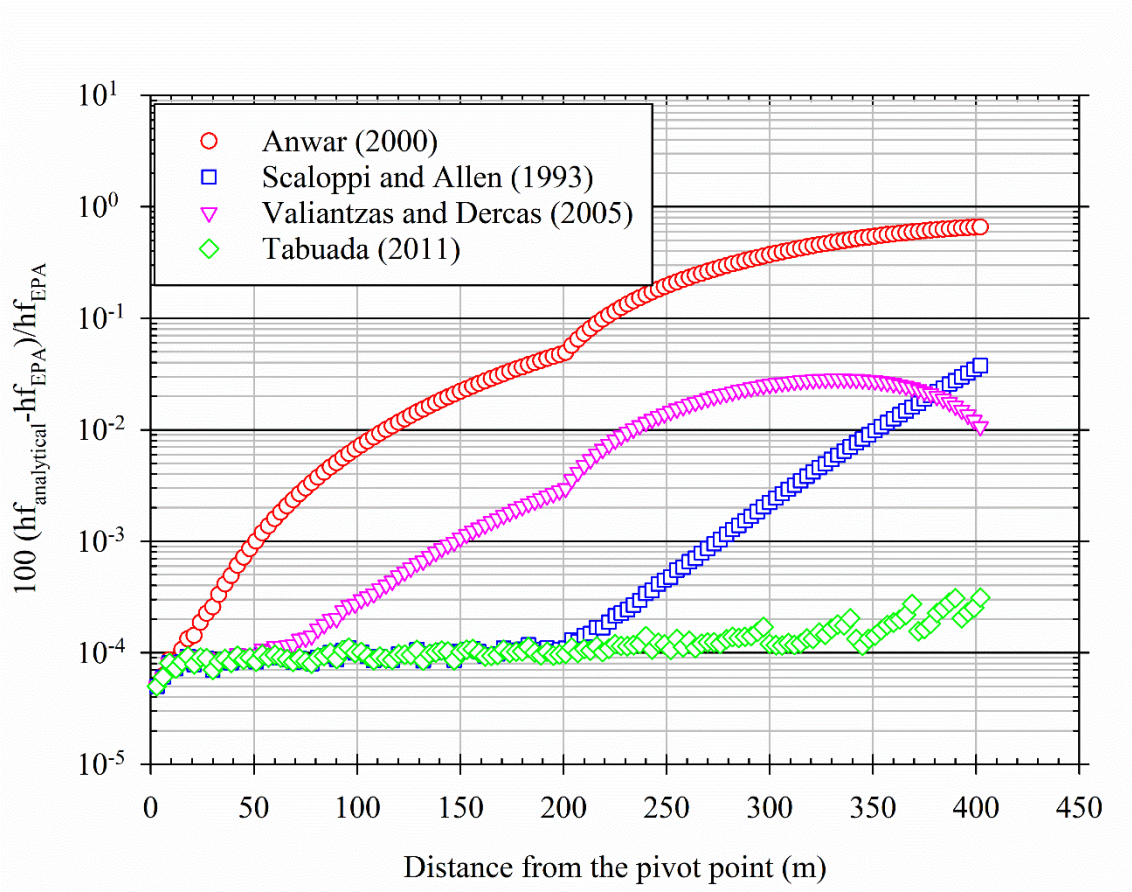

Fig. 3. Relative deviations of estimates of accumulated head loss along one center pivot lateral line in relation to EPANET 2.0 (L_T = 402 m; L_U = 201 m; D_U = 0.168 m; D_D = 0.127 m, C_{HW} = 135; d_G/T_c = 5 mm/24 h; gr = 0.2).

It is possible to observe in Fig.3 that the estimates of accumulated head loss provided by the solution of Valiantzas and Dercas (2005) present absolute deviations lower than those provided by the solution of Scaloppi and Allen (1993a) only in the final segment of lateral. The performance of the solution proposed by Scaloppi and Allen (1993a) worsens as the distance to the pivot point increases. The solution proposed by Scaloppi and Allen (1993a) presents performance similar to those obtained by the hard-working solution proposed by Tabuada (2011) for relative values of distance to the pivot point (x/L_T) lower than 0.5.

Pressure head distribution with analytical methods and EPANET 2.0

Pressure head spatial distributions equation along a center lateral with the nineteenth configuration presented in Table 1, under two different ground slope values (S_0 = 0 and S_0 = -0.02) are presented in Fig. 4. Head loss values were computed based on the Darcy-Weisbach equation.

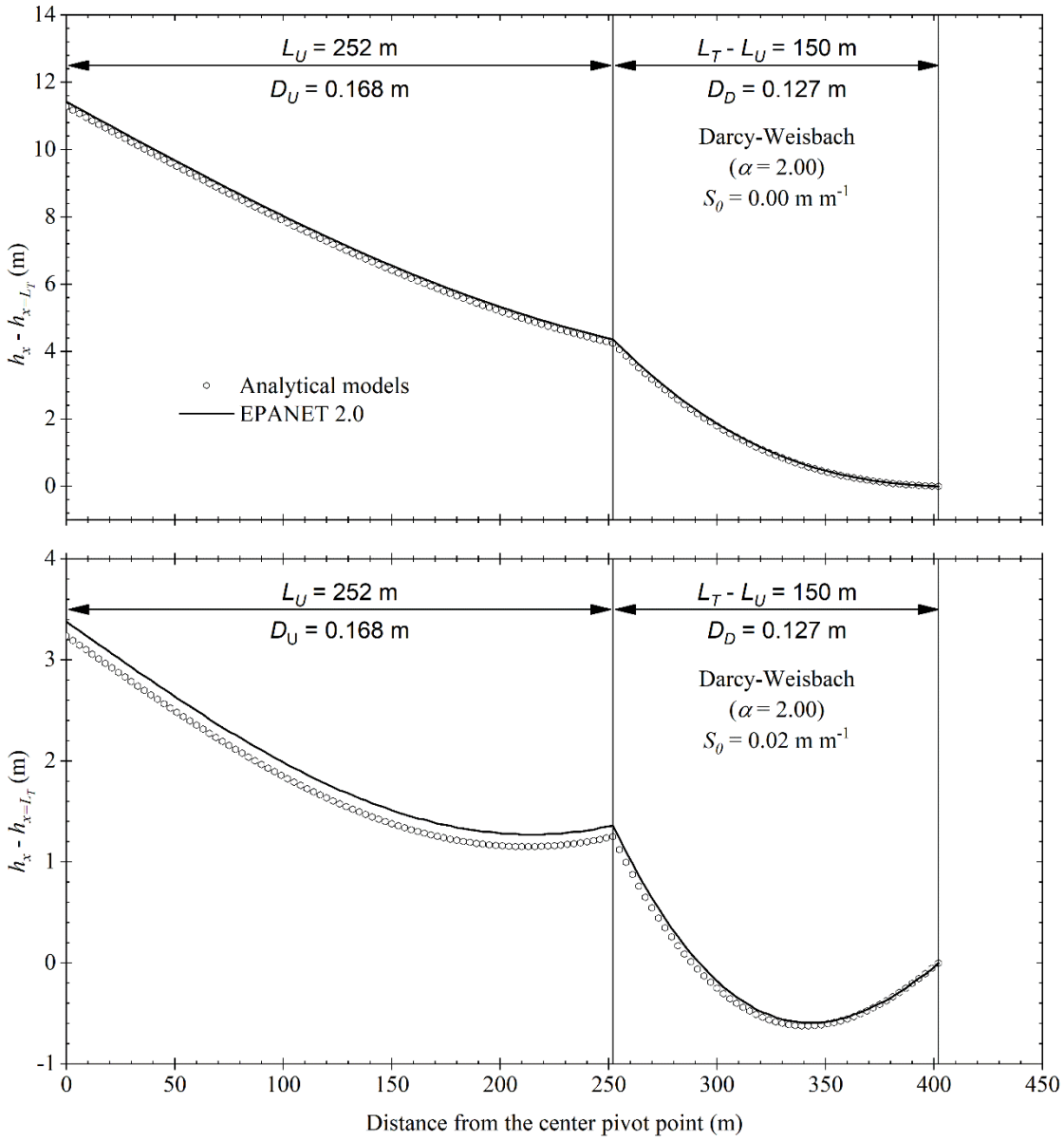

Fig. 4. Pressure head profiles along two-diameter center pivot lateral (Darcy-Weisbach equation)

As demonstrated before, when the Darcy-Weisbach equation with α = 2.0 is used, all head loss correction factors (Eqs. (10), (11), (12) and (14)) present the same value (Table 2), consequently, all four analytical models considered in this study presented the same deviation values in relation to the head loss values obtained with the numerical method used by the hydraulic simulator EPANET 2.0. Similar deviations among pressure head values predicted by analytical models and pressure head values predicted method were also reported by Valiantzas and Dercas (2005), in a study on hydraulic analysis of central pivot lateral lines with different diameters.

As indicated in Fig. 5, when the pressure head spatial distribution of the same lateral lines considered in Fig. 4, were computed using the Hazen-Williams equation (α = 1.852), all four analytical models presented different results.

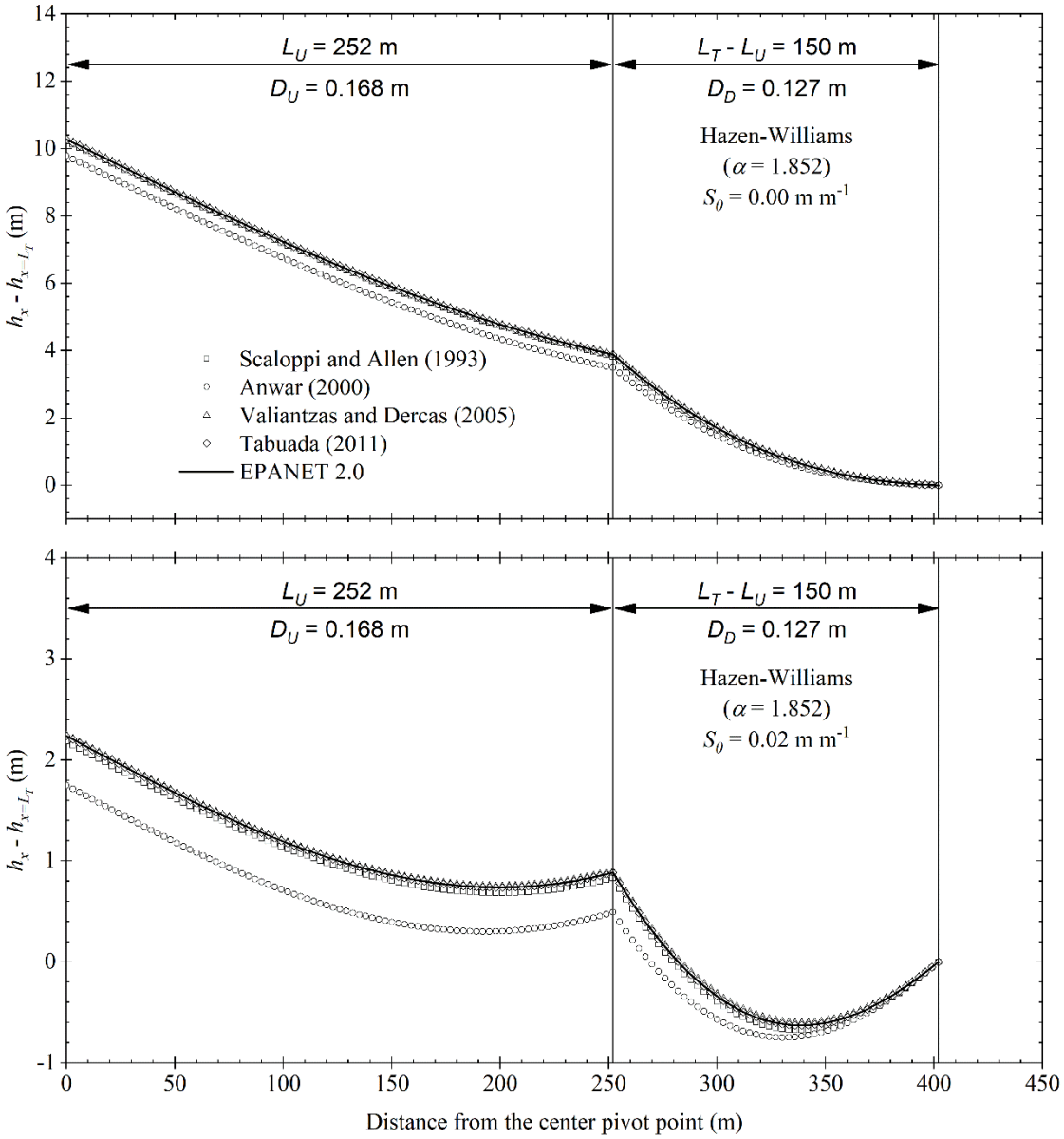

Fig. 5. Pressure head profiles along two-diameter center pivot lateral (Hazen-Williams equation)

This fact was expected, since as indicated in Tables 3 and 4, for the same lateral line configuration, all four analytical models presented different values of total head loss along the center pivot lateral line. Due the fact that the Anwar (2000) model assumes a constant value for exponent (α) equal to 2.0, the differences among pressure head values predicted by this

analytical model and the numerical model (EPANET 2.0) was greater than the differences among the other three analytical models and the numerical model (EPANET 2.0).

Conclusions

The four analytical solutions assessed in the current work to estimate head loss values similar to those obtained by the numerical process (EPANET 2.0). Those results indicate that the very time-consuming process required to describe the flow rate distribution along a center pivot lateral line that is required by numerical methods does not improve the accuracy of the results obtained with the simple continuous description of lateral line flow distribution assumed by the four analytical models assessed in the current work.

When Darcy-Weisbach equation (α = 2.0) is used, the solution of Anwar (2000) is recommended, since the greatest mathematical complexity of the other three analytical models does not improve the accuracy of the obtained results. When Hazen-Williams equation is used with α = 1.852, the lowest deviations in relation to the numerical model (EPANET 2.0) were observed with the analytical solution proposed by Tabuada (2011). At radial distances near the lateral line inlet, head loss values predicted by the solution, proposed by Scaloppi and Allen (1993a), presented smaller deviation in relation to values predicted by the EPANET than the values predicted by the solution proposed by Valiantzas and Dercas (2005). However, with increasing values of distance to the lateral line inlet head loss values predicted by the Valiantzas and Dercas (2005) model presented smaller deviation in relation to values predicted by the EPANET 2.0 than the values predicted by Scaloppi and Allen (1993a).

Data Availability Statement

All data, models, and code generated or used during the study appear in the submitted article.

Notation

The following symbols are used in this paper:

$F_{L_U}^{\lambda}$ = center pivot head loss distribution correction factor for the radial distance L_U.

hfd_x = pipe friction head loss for dual-diameter between the center pivot lateral line inlet and the radial distance x

hf_x = pipe friction head loss between the center pivot lateral line inlet and the radial distance x

hf_x^{λ} = pipe friction head loss between the center pivot lateral line inlet and the radial distance x estimated with the analytical model identified by the λ index

F_x^{λ} = center pivot head loss distribution correction factor for the radial distance x

h_x^{λ} = pressure head at radial distance x from the pivot point estimated by the analytical model identified by the λ index

Sf_{D_U} = head loss per unit length of a pipe with inner diameter D_U conducting the center pivot lateral line inlet discharge Q_0

Sf_{D_D} = head loss per unit length of a pipe with inner diameter D_D conducting the center pivot lateral line inlet discharge Q_0

B_{in} = incomplete beta function

C_{HW} = friction coefficient for the Hazen–Williams equation

D = center pivot lateral line inner diameter (D_U or D_D)

d_G = gross irrigation depth

f = friction coefficient of the Darcy–Weisbach equation

F_{hyper} [ ] = hypergeometric function

g = gravitational acceleration

gr = end gun ratio

h_0 = pressure head at the pivot point

i = number of lateral line water outlets

JPP = junction name of lateral line water inlet

L_{Eq} equivalent hydraulic length of a center pivot lateral line

L_T = physical length of the center pivot lateral line

L_U = upstream lateral line length

Q_0 = total flow rate at the inlet of the center pivot lateral with a value that corresponds to the sum of the discharge rate of all center pivot outlets, including the end gun discharge rate

q_i = flow rate (*base demand in EPANET 2.0*) with order number i ($1 \leq i \leq 134$)

Q_x = flow rate at point x;

S_0 = constant slope of the ground elevation

Sf_D = head loss per unit length of a pipe with inner diameter D conducting the center pivot lateral line inlet discharge Q_0

Ss = uniform outlet spacing

T_c = time period required for a complete lateral line revolution

V1E134 = name of the last lateral line water outlet

V1Ei = lateral line water outlets names

V1Li = lateral line pipe segment names

x = distance taken from the lateral line inlet at the pivot point

X, Y = EPANET 2.0 hydraulic network map graphical coordinates

α = flow rate exponent in the head loss equation (α= 1.852 for Hazen-Williams, or α= 2.0 for Darcy–Weisbach)

ε = pipe wall absolute roughness

θ = integration variable equal to $(s/L_{Eq})^2$

λ = index used in identifying the head loss equation (λ = S, A, V, or T)

Acknowledgments

We would like to thank the Coordenação de Aperfeiçoamento de Pessoal de Nível Superior - Brasil (CAPES) – PDSE process number 88881.190146/2018-01; and CNPq for the scholarships awarded.

References

Allen, R. G., Keller, J., and Martin, D. L. (2011). *Irrigation Association: Center Pivot Design*. Saint Joseph: ASAE.

Anwar, A. A. (2000). "Correction Factors for Center Pivots with End Guns." *Journal of Irrigation and Drainage Engineering*, 126(2), 113–118.

Brar, D., Kranz, W. L., Lo, T., Irmak, S., and Martin, D. L. (2017). "Energy Conservation Using Variable-Frequency Drives for Center-Pivot Irrigation: Standard Systems." *Transactions of the ASABE*, 60(1), 95–106.

Brar, D., Kranz, W. L., Lo, T., Irmak, S., and Martin, D. L. (2019). "Energy Conservation using Variable Frequency Drivas for Center-Pivot Irrigation Systems Equipped with Corner Watering Attachments." 62(5), 1395–1408.

Chandrupatla, T., and Osler, T. (2010). "The perimeter of an ellipse." *Math. Scientist*.

Chu, S. T., and Moe, D. L. (1972). "Hydraulics of a Center Pivot System." *Transactions of*

the ASAE, 894–896.

Córcoles, J. I., Tarjuelo, J. M., and Moreno, M. A. (2016). "Methodology to improve pumping station management of on-demand irrigation networks." *Biosystems Engineering*, 144, 94–104.

Fernández García, I., Montesinos, P., Camacho Poyato, E., and Rodríguez Díaz, J. A. (2017). "Optimal Design of Pressurized Irrigation Networks to Minimize the Operational Cost under Different Management Scenarios." *Water Resources Management*, Water Resources Management, 31(6), 1995–2010.

García-González, J. F., Moreno, M. A., Molina, J. M., Madueño, A., and Ruiz-Canales, A. (2015). "Use of software to model the water and energy use of an irrigation pipe network on a golf course." *Agricultural Water Management*, 151, 37–42.

Moreno, M. A., Planells, P., Ortega, J. F., and Tarjuelo, J. M. (2008). "Calibration of On-Demand Irrigation Network Models." *Journal of Irrigation and Drainage Engineering*, 134(February), 36–42.

Rossman, L. A. (2000). "EPANET 2: User Manual." *Cincinnati US Environmental Protection Agency National Risk Management Research Laboratory*, (September), 104.

Sadeghi, S. H., and Peters, T. (2013). "Adjusted friction correction factors for center-pivots with an end-gun." *Irrigation Science*, 31(3), 351–358.

Scaloppi, E. J., and Allen, R. G. (1993a). "Hydraulics of Center Pivot Laterals." *Journal of Irrigation and Drainage Engineering*, 119(3), 554–567.

Scaloppi, E. J., and Allen, R. G. (1993b). "Hydraulics of Irrigation Laterals: Comparative Analysis." *Journal of Irrigation and Drainage Engineering*, 119(1), 91–115.

Swamee, P. K., and Jain, A. K. (1976). "Explicit Equations for Pipe-Flow Problems." *Journal of the Hydraulics Division - ASCE*, 102, 657–664.

Tabuada, M. A. (2011). “Friction Head Loss in Center-Pivot Laterals with Single Diameter and Multidiameter.” *Journal of Irrigation and Drainage Engineering*, 140(10), 04014033.

Tabuada, M. A. (2014). “Friction Head Loss in Center-Pivot Laterals with the Lateral Divided into Several Reaches.” *Irrigation & Drainage Systems Engineering*, 2(1).

Valiantzas, J. D. (2005). “Modified Hazen–Williams and Darcy–Weisbach Equations for Friction and Local Head Losses along Irrigation Laterals.” *Journal of Irrigation and Drainage Engineering*, 131(August), 342–350.

Valiantzas, J. D., and Dercas, N. (2004). “Economic Design of Center-Pivot Sprinkler Laterals.” *Journal of Irrigation and Drainage Engineering*, 130(6), 491–498.

Valiantzas, J. D., and Dercas, N. (2005). “Hydraulic Analysis of Multidiameter Center-Pivot Sprinkler Laterals.” *Journal of Irrigation and Drainage Engineering*, 131(2), 137–146.

ARTICLE 2 - FEASIBILITY OF THE USE OF VARIABLE SPEED DRIVES IN CENTER PIVOT SYSTEMS INSTALLED IN PLOTS WITH VARIABLE TOPOGRAPHY

Article elaborated according to standards of the scientific journal *Water*, ISSN: 2073-4441 (Water 2019, 11, 2192; doi: 10.3390/w11102192)

Article

Feasibility of the Use of Variable Speed Drives in Center Pivot Systems Installed in Plots with Variable Topography

Victor Buono da Silva Baptista [1], Juan Ignacio Córcoles [2], Alberto Colombo [3] and Miguel Ángel Moreno [4,*]

[1] Engineering Dept., University of Lavras. Campus Universitario, s/n, 3037 Lavras, Brazil; victor.buonosb@ufla.br
[2] Renewable Energy Research Institute, Section of Solar and Energy Efficiency, C/ de la Investigación 1, 02071 Albacete, Spain; JuanIgnacio.Corcoles@uclm.es
[3] Water Resources and Sanitation Dept., University of Lavras. Campus Universitario, s/n, 3037 Lavras, Brazil, acolombo@ufla.br
[4] Institute for Regional Development, University of Castilla-La Mancha. Campus Universitario, s/n, 02071 Albacete, Spain
* Correspondence: MiguelAngel.Moreno@uclm.es
Received: 11 September 2019; Accepted: 17 October 2019; Published: 21 October 2019

Abstract: Pumping systems are the largest energy consumers in center pivot irrigation systems. One action to reduce energy consumption is to adjust the pumping pressure to that which is strictly needed by using variable speed drives (VSDs). The objective of this study was to determine the feasibility of including VSDs in pumping systems that feed center pivot systems operating in an area with variable topography. The VSPM (Variable Speed Pivot Model) was developed to perform hydraulic and energy analyses of center pivot systems using the EPANET hydraulics engine. This tool is able to determine the elevation of each tower for each position of the center pivot using any type of digital elevation model. It is also capable of simulating, in an accurate manner, the performance of the center pivot controlled with a VSD. The tool was applied to a real case study, located in Albacete, Spain. The results show a reduction in energy consumption of 12.2%, with specific energy consumptions of 0.214 and 0.244 kWh m^{-3} of distributed water obtained for the variable speed and fixed speed of the pumping station, respectively. The results also show that for an irrigation season, to meet the water requirements of the maize crop in the region of the study (627 mm), an average annual savings of 14,107.35 kWh was obtained, which resulted in an economic savings of 2821.47€.

Keywords: hydraulic model; variable topography; energy consumption; variable speed; center pivot system

1. Introduction

The quantity and quality of food needed to satisfy all the demands of the population will become a major concern worldwide in the following years. It is expected that by the year 2050, there will be a world population of 9.15 billion people [1]. The increase of food production to satisfy demand is a challenge for agricultural professionals, who require the use of techniques focused on increasing production efficiency. Increasing use efficiency in food production requires the use of improved technology in all production processes, as well as improving the efficiency of irrigation systems.

Irrigated agriculture accounts for 16% of the world's cultivated area and is expected to produce 44% of world food by 2050 [1–3].

Sustainable use of water resources could be accomplished increasing the efficiency of irrigation systems, thereby reducing the amount of water and energy to satisfy crop water requirements. In this regard, technological developments in the infrastructures of irrigation systems contribute to increasing water use efficiency. However, this efficiency increase is related to a significant increase in energy consumption in recent years [4].

According to [5], sprinkler irrigation systems represent around 11% (35 million hectares) of the total irrigated areas in the world. Within this method, the most outstanding systems are conventional sprinklers, traveling guns, center pivots, and linear-moving laterals. With eight million hectares of irrigated area, the center pivot system represents 23% of the area irrigated by sprinkler irrigation systems.

Center pivot irrigation consists of the application of water through a moving lateral line with several water outlets supported on moving towers, which revolve around a fixed pivot point (center tower) and irrigate a circular area [6,7]. This equipment is considered a highly efficient system compared to other irrigation systems. It is flexible and easily operable, which reduces labor and maintenance costs. It can also be operated on surfaces with variable topography, resulting in conservation of water, energy, and time [8]. However, the initial cost of the equipment and the required energy demands at the pumping station are some of its main limitations.

The reduction of the energy consumption of pumping stations that feed irrigation systems has been studied by several researchers. Pumping stations are the largest consumers of energy in pressurized irrigation systems, especially in situations where underground water resources are used.

Gilley and Watts (1977) [9] suggested several changes in center pivot systems: switching high and medium pressure sprinklers to low pressure emitters, changing nozzle size and spacing, or changing irrigation intervals and maintenance to increase pumping station efficiency. Moreno et al. (2008) [10] developed a new methodology to obtain the characteristic curves of the pump, thereby minimizing the costs of the pumping station. In a later study, [11] stated that the energy consumption of the center pivot, which irrigates an area of 75 ha, can be minimized by adopting measures like increasing the lateral line's diameter, reducing the equipment's operating time, and increasing the flow per unit of area. Barbosa et al. (2018) [12] concluded that constant center pivot monitoring is essential to maintaining adequate energy efficiency levels when assessing the behavior of different energy efficiency indicators for a center pivot operating in variable topography.

In center pivot equipment, the pumping station is designed to meet the most critical situation, i.e., the position of the lateral line where there is the highest elevation point and the greatest need for higher pumping pressure [13]. However, this situation is variable along with the lateral line rotation in the irrigated area due to topographic differences. This means that the pumping station is oversized during most of the lateral line rotation, and the energy is wasted. Pressure regulating valves are installed before the emitters, so pressure fluctuations that are due to topographical differences and oversizing of the pumping station do not influence the flow rate of the emitters [14].

An option to adjust the pumping pressure of this equipment is the use of variable speed drives (VSDs) to control the speed of these pumps [15,16]. This control provides a substantial reduction in power in relation to the reduction of flow and pressure in pressurized irrigation systems [13,17].

Several researchers have used variable speed drives to control pumping stations to reduce energy consumption. Hanson et al. (1996) [18], in a center pivot system with a well pumping unit, concluded that variable speed pumps save about 32% of the energy. Lamaddalena and Khila (2012) [19] showed that 27% to 35% of energy savings can be achieved using VSD in two Italian irrigation districts operating with three parallel horizontal axis pumps. Brar et al. (2017) [20] concluded that a 9.6% energy reduction is possible for a 13.6 m difference in the irrigated area for a study containing 100 center pivots in Nebraska (USA), with each pivot containing a pumping station. In this study, digital

elevation models (DEMs) with a spatial resolution of 10 m × 10 m were used to obtain the topographic characteristics of the irrigated areas.

King and Wall (2000) [13] stated that the optimum efficiency in terms of energy and water use can be achieved when the pumping station is able to maintain the required minimum pressure regardless of the operating conditions. Scaloppi and Allen (1993) [21] stated that the point of minimum pressure is constantly moving along the lateral line because it is influenced by the topography of the irrigated area. They also presented theoretical bases for the calculation of this movement.

However, working with the minimum pressure does not always guarantee the lowest power consumption due to variations in the operating point of the pump and variable performance when working at low frequencies [17,22]. In addition, most of these studies did not take into account the effect of the VSD efficiency on the final result. Therefore, it is important to consider VSD efficiency in energy savings accounting and not assume that this efficiency will always be constant and high [17].

In a study on VSD efficiency, [13] reported that a pumping station with a VSD can save 15.8% and 20.2% of its energy compared to fixed speed pumping (for uniform and variable rate irrigation, respectively) without considering the inefficiency of the VSD. When the efficiency of the VSD is accounted for, there are 7.5% and 12.4% energy savings, respectively.

The main novelty of the present study is developing a simulation model of hydraulic behavior by considering the hydraulic elements of the irrigation system in detail and integrating the energy characteristics of the pumping station and topographic characteristics through digital elevation models (DEMs). In this way, energy efficient technologies and management strategies can be developed to reduce energy use to ensure sustainable irrigation without reductions in the efficiency of water application.

The objective of the present study was to determine the feasibility of including variable speed drives in pumping systems that feed center pivot irrigation systems operating in areas with variable topography. Considering this objective, the VSPM (Variable Speed Pivot Model) tool was developed, in which the hydraulic simulation model of the pivot was integrated into a simulation model of the pumping station so that, with data related to topography, flow rate, and pressure, the power supply could be adjusted to the actual demand of the system. In addition, it is useful to determine the potential of reduction from the perspective of the energy, economics, and sustainability of the installation of the VSDs in these irrigation systems.

2. Material and Methods

2.1. Proposed Procedure

The proposed methodology has the following steps, as presented in 1. For the development of this model and data acquisition, a real center pivot was used. However, this model can be used for pivots of different sizes and with different numbers of towers.

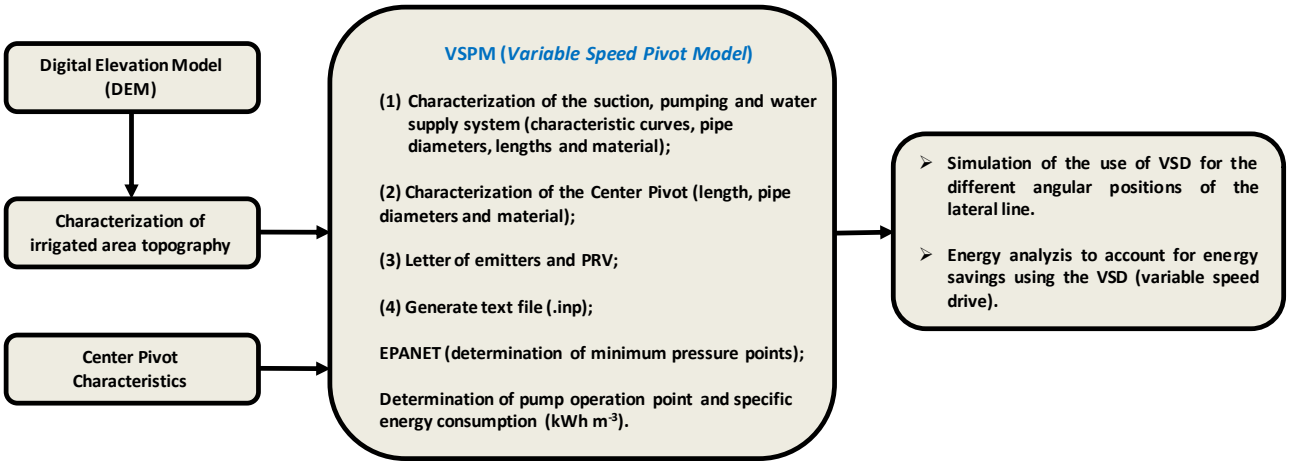

Figure 1. Diagram of the proposed procedure.

The characterization of the irrigated area, along with the characteristics of the pumping station and irrigation system from the manufacturers' technical data, were inserted into the VSPM (Variable Speed Pivot Model) tool to process and edit the input data. Subsequently, the hydraulic simulation was calculated using the EPANET hydraulic engine. The hydraulic simulation results were then used to determine the energy consumption of the irrigation system under study.

2.2. Topography of the Irrigated Area

As shown in Figure 1, the elevation values of the moving towers were obtained through Digital Elevation Models (DEMs) (with a spatial resolution of 5 m × 5 m), which were freely obtained from the PNOA (Spanish National Program of aerial photogrammetry). These products are freely available for any location in Spain. The developed tool is able to use any type of DEM.

The utilized DEMs (.tif formatted images) were loaded into the QGIS® Desktop 3.2.1 software (QGIS Development Team, Open Source Geospatial Foundation). In this software, the geographical coordinates (X, Y) of the point referring to the center of the pivot (X_0, Y_0) were defined.

To obtain the X and Y coordinates of all moving towers in different angular positions relative to the center pivot's lateral line, a computational routine was developed in the MATLAB® 2018b software. Automatically, with the values of the geographic coordinates and the distance between towers, the elevation values were determined for 36 angular positions of the lateral line, equally spaced by 10°, with the North position of the lateral line as the position of angle 0°, as in Figure 2.

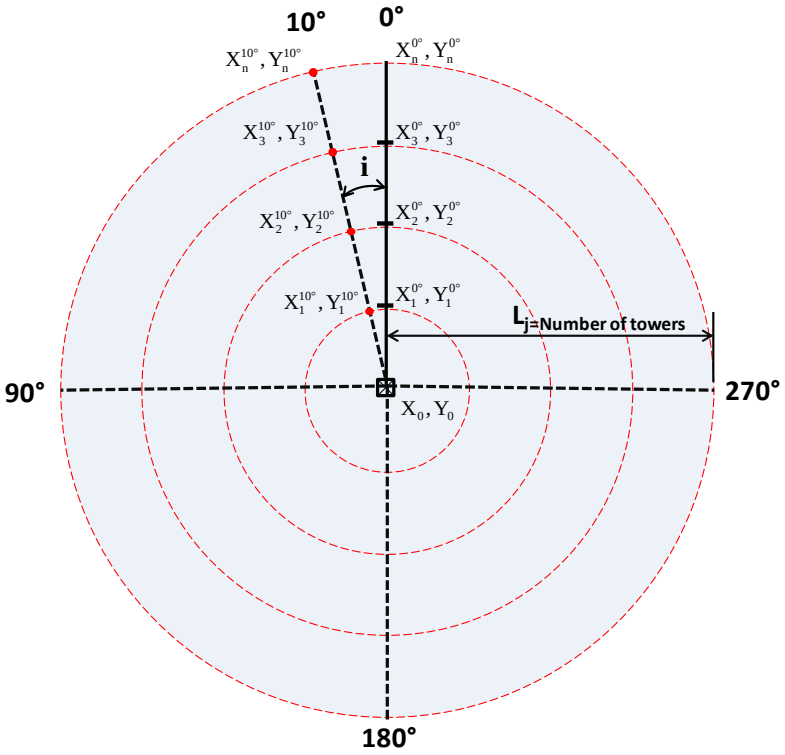

Figure 2. The geographic coordinates during the rotation of the lateral line at the center pivot.

The calculation of the geographical coordinates X, Y of each moving tower (j) was carried out as follows:

$$X_j^i = X_0 + L_j \cdot \cos(i) \text{, with } 1 \le j \le \text{Number of towers} \quad (1)$$

$$Y_j^i = Y_0 + L_j \cdot \sin(i) \text{, with } 1 \le j \le \text{Number of towers} \quad (2)$$

where i is the angular position of the lateral line (0°, 10°, ..., 350°), j is the number of moving towers, in this case, $1 \le j < \le 9$, and L_j is the distance from the center tower to the index tower j, m.

Thus, for the center pivot under study, the dimensions of the nine moving towers were obtained in 36 different angular positions of the lateral line, resulting in 324 elevation values.

2.3. Hydraulic Model Description

The simulation of the operation of the center pivot irrigation system, for different angular positions of the lateral line of the center pivot, was carried out using EPANET software [23]. With this aim, the VSPM tool was developed. The function of this tool is to edit the input data required by the EPANET software in addition to energy analysis, as shown in Figure 1.

Center pivot irrigation system simulations, for different lateral line angular positions, was carried out using EPANET software [23]. With this aim, the VSPM tool was developed. The function of this tool is to edit the input data required by the EPANET software in addition to energy analysis, as shown in Figure 1. Figure 3a shows the dimensions of the lateral line span and Figure 3b shows the EPANET network map of the first span of the center pivot lateral line.

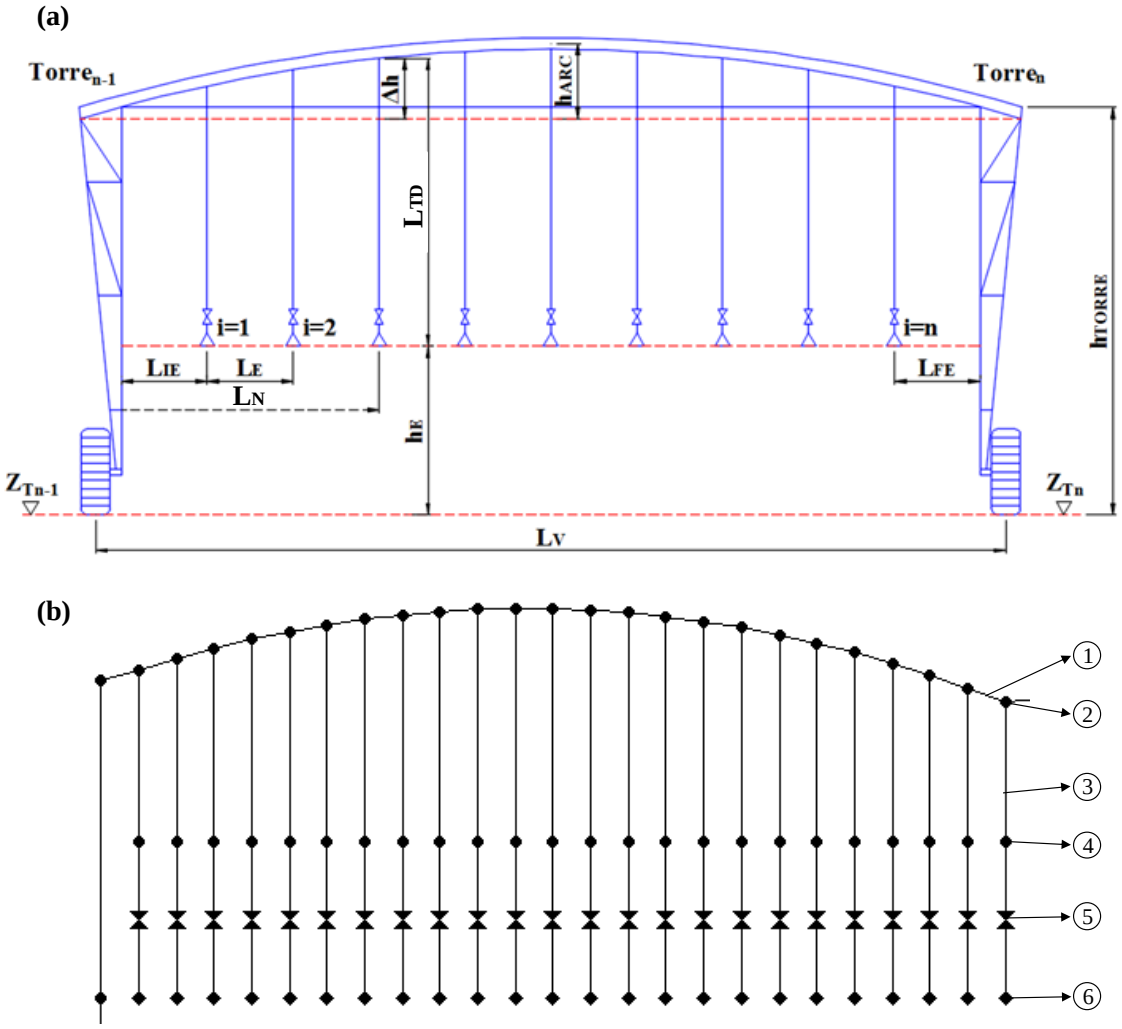

1 – Lateral line pipe;
2 – Lateral line node;
3 – Drop pipe;
4 – Drop pipe node;
5 – Pressure Regulator Valve;
6 – Emmiter.

Figure 3. (**a**) Center pivot lateral line span dimensions, (**b**) EPANET network map of the first span of the center pivot lateral line.

The VSPM tool has four steps: (1) characterization of the suction, pumping, and water supply systems, (2) characterization of the center pivot, (3) emitters and pressure regulating valves (PRV), (4) generation of the text file in the EPANET format.

The system that includes suction, pumping, and water supply was pre-determined containing the following hydraulic elements: a fixed level reservoir (water source), a pumping station, and a supply pipe composed of three different links. The required information for these components are: elevation of the water level in the reservoir, elevation of the ground where the pumping station is located, length, pipe diameter and roughness coefficient (depending on the selected head loss equation) of all links, and the pairs of values (Q-H) constituting the pump characteristic curve, as taken from the manufacturer's technical data.

In the center pivot characterization module, the center pivot's equipment information is inserted: the elevation of the pivot point and the elevation of the moving towers, as well as pipe lengths, pipe diameters, and the roughness coefficient of the pivot point, lateral line, and drop pipes.

In the module related to emitters and pressure regulating valves (PRVs), the emission coefficients of the emitters and the working pressure of the PRVs are inserted. If information about the emitter's distribution on the pivot is not available, it remains possible to generate and simulate a commonly used commercial emitter distribution with this tool.

Finally, the VSPM tool generates a text file (in .inp format) with all the hydraulic model information entered by the user. This file consists of input data, which is required by EPANET to perform the hydraulic simulation. In the VSPM modules, the flow rate and discharge coefficient of each emitter, the node elevations, and the pipe lengths were determined.

2.3.1. Flow Rate of the Emitters

The total flow of the irrigation system is the sum of the flow rate of each emitter along the lateral line. The flow rate of the emitters (in $m^3\ h^{-1}$) was calculated according to the area corresponding to each water outlet, and the gross depth to be applied to the rotation time was specified by the manufacturer, as proposed by [24]. The flow rate for the first outlet of each span (Equation 3) and the remainder of each outlet (Equation 4) was calculated. The lengths used are shown in Figure 3a:

$$q_{x=1} = \frac{2\pi L_{IE}^{\ 2}}{1000}\frac{Lb}{Tg}, \text{ for } x = 1 \quad (3)$$

$$q_x = \frac{2\pi R_{inst} L_E}{1000}\frac{Lb}{Tg}, \text{ for } 2 \le x \le n \quad (4)$$

where q_x is the flow rate of the outlet with order number x ($1 \le x \le n$), $m^3\ h^{-1}$, L_{IE} is spacing between the tower and the first emitter (x = 1), m, L_E is the spacing between the emitters with order number x ($2 \le x \le n$), m, R_{inst} is the radius of the installation of the emitter, relative to the center tower, m, Lb is the gross irrigation depth (9 mm), and Tg is the rotation time (21 hours).

After the acquisition of the flow rate values at each water outlet (q_x), the discharge coefficient (k_e, Equation 5) of each emitter was determined. The value of the pressure in the emitter was the same as the value of the PRV nominal pressure (H_{prv}), assuming an ideal valve:

$$k_e = \frac{q_i}{H_{prv}^{\ \beta}} \quad (5)$$

Where k_e is emitter discharge coefficient, $m^{2.5}\ h^{-1}$, H_{prv} is the PRV nominal pressure, m, and β is the pressure exponent, in this case with a value of 0.5.

2.3.2. Determination of Elevations and Lengths

The spans lengths (Equation 6) and the water outlet relative distance to the previous moving tower (Equation 7) were calculated:

$$L_S = L_{IE} + L_{FE} + \left[\left(N_O - 1\right) L_E\right] \quad (6)$$

$$L_N = \begin{cases} N = 1 \Rightarrow R_T + L_{IE} \\ 2 \le N < n \Rightarrow L_{N=1} + L_E \\ N = n \Rightarrow L_{2 \le N < n} + L_{FE} \end{cases} \quad (7)$$

where L_S is the length of span (m), L_{FE} is the distance between the last emitter and next tower of the span (m), N_O is the number of water outlets in the span, L_N is the distance of the node referring to the water outlet in relation to the previous tower (m), N is the water outlet in the span, and R_T is the radius of rotation of the tower relative to the centre tower (m).

The irrigation system is composed of nodes, which are the connections between the links. Each water outlet was determined as a set of six hydraulic components, as shown in Fig 3b. Elevation is the main feature required for the nodes (Equation 8). The slope between the towers (Equation 9), the variable height between the lateral line and the height of the tower (Equation 10), and the length of the drop pipe (Equation 11) were also calculated:

$$Z_{n=x} = Z_{Tn-1} + \left(S_T L_N\right) + \Delta h \tag{8}$$

$$S_T = \frac{Z_{Tn} - Z_{Tn-1}}{L_S} \tag{9}$$

$$\Delta h = \frac{4 h_{arc} L_N^{\,2}}{L_S^{\,2}} \left(\frac{L_S}{L_N} - 1 \right) \tag{10}$$

$$L_{DP} = h_T - h_E + \Delta h \tag{11}$$

where $Z_{n=x}$ is the node elevation x, m. Z_{Tn-1} is the tower elevation previous to node n (m). Z_{Tn} is the tower elevation posterior to node n (m). S_T is the slope between towers n e n-1. ⌀h is the length of the drop pipe between the lateral line and the tower are variable for each lateral line water outlet (m). h_{arc} is the maximum height of the lateral line arc (m). L_{DP} is the total length of the drop pipe, which is variable for each lateral line water outlet (m). h_T is the height of the moving towers (m). h_E is the height of the emitter relative to the ground (m).

For the case of the overhanging nodes, the same slope (S_T) of the last span of the lateral line was assumed in the calculation of the dimensions ($Z_{n=x}$).

2.4. Calculation of the Pumping Operation Point and Energy Consumption

2.4.1. Hydraulic Model

Using EPANET, the hydraulic simulation was performed at each angular position of the center pivot lateral line with the pumping station operating at a maximum fixed speed. The head loss was computed based on the Hazen–Williams roughness coefficient (C_{HW}) values of 100 (for the lateral line and water supply pipe) and 140 (for drop pipes).

Head and efficiency curves of the pump are considered. Affinity laws were implemented to the regulation of variable frequency drive. For an accurate analysis of the efficiency, all the components of the pumping station were considered, as proposed by [17]. Also, energy losses in cables were computed.

$$\eta_t = \eta_p \cdot \eta_m \cdot \eta_v \cdot \eta_c \tag{12}$$

Where η_t is the total efficiency of the pumping station, η_p is the pump efficiency, η_m is the motor efficiency, η_v is the VSD efficiency, and η_c is the cable efficiency.

The motor efficiency for each angular position i was determined through the exponential model proposed by [25].

$$\eta_{m_i} = 0.94187 \cdot \left(1 - e^{-0.0904 \cdot \left(\frac{P_{Abs(i)}}{P_{Nom}} \right)} \right) \tag{13}$$

Where P_{Nom} is the nominal power in kW and $P_{Abs(i)}$ is the absorbed power in kW.

To compute the VSD efficiency values at each angular position i of the lateral line, Equation 14 was used. This value should be supplied by the VSD manufacturer but is commonly not supplied. In this case study, we utilized the value obtained by [22] for a pump with a similar power:

$$\eta_{v_i} = 70.126 - 232.47\alpha + 582.032\alpha^2 - 323.134\alpha^3 \quad (14)$$

Where α is the ratio between the speed of the variable speed drive and the maximum speed as a fixed speed drive (n_v/n_f)

2.5. Determination of Specific Energy Consumption (CEE)

At each angular position of the lateral line (36 angular positions spaced 10°) the minimum pressure required to pressurize the irrigation system was determined. Therefore, at each position, the adequate pumping pressure head (H_i) was estimated:

$$H_i = H_p - \left(H_{min(i)} + H_{prv}^{*}\right) \quad (15)$$

Where H_P is the pressure head at the fixed pumping speed (m), $H_{mín(i)}$ is the minimum pressure head along the lateral line at each angular position i, m (obtained in EPANET), and H_{prv}^{*} is the PRV pressure head, including the pressure regulator loss (69 kPa + 34 kPa).

The specific energy consumption using the VSD at each angular position i of the lateral line (CEE_i^v, em kWh m^{-3}, Equation 16) for 0° ≤ i ≤ 350° was calculated by the values of the pumping pressure head (H_i, m), the water specific weight (γ, N m^{-3}), and the efficiencies (η) of the pump, motor, VSD, and cable:

$$CEE_i^v = \frac{H_i\ \gamma}{3600\ (\eta_{b_i}\ \eta_{m_i}\ \eta_{v_i}\ \eta_{c_i})} \quad (16)$$

The specific energy consumption of the equipment, considering a pumping station with a fixed speed (CEE^f, em kWh m^{-3}), was determined through Equation 17:

$$CEE^f = \frac{H_p\ \gamma}{3600\ (\eta_b\ \eta_m\ \eta_c)} \quad (17)$$

The energy reduction (ER, %) was determined by Equation 18. The energy consumption (EC, kWh) in the pump station for each position (fixed speed and variable speed) was determined from Equations 19 and 20, respectively.

$$ER = \left(\frac{CEE^f - \left(CEE_i^v\right)_{av}}{CEE^f}\right) \times 100 \quad (18)$$

$$EC_f = Q \times T_0 \times CEE^f \quad (19)$$

$$EC_v = Q \times T_o \times \left(CEE_i^v\right)_{av} \quad (20)$$

Where $(CEE_i^v)_{av}$ is the average of the specific energy consumption in the different angular positions of the lateral line, and T_o is the operating time of the irrigation system.

2.6. Case Study

This study was developed in a center pivot irrigation system located in the "La Felipa" district, which belongs to Chinchilla de Monte-Aragón (Albacete) in the Castilla La-Mancha region (Spain). The geographical coordinates of the latitude and longitude of the center point of the pivot are 39° 4'44.43" N and 1°39'35.27" W. The elevations of the water level in the reservoir, the pumping station, and the center pivot point are, 675.91 m, 676.91 m, and 661.91 m, respectively

With regard to the center pivot, the lateral line of this equipment operates without an end gun, irrigating an area with a total radius of 488.6 m, equivalent to a surface area of 76 ha. The lateral line is composed of nine spans, comprising four spans with a length of 57 m, five spans with a length of 51 m, and an overhang of 5.6 m. The lateral line has an internal pipe diameter of 162.27 mm to the last tower, and the overhang has an internal pipe diameter of 108.74 mm. Along the lateral line, there are 164 emitters (type SP4 + PL / R), which are all equipped with pressure regulator valves (69 kPa) that have a pressure regulator loss of 34 kPa, with 3 m spacing. The first outlet is located 2.10 m from the pivot point, mounted at the end of flexible drop pipes, with an internal pipe diameter of 19.05 mm at a height of 1.80 m from the ground surface. The towers have a fixed height of 3.54 m, and the largest arc of the spans has a value of 0.7 m in height. The highest elevation of the irrigated area is 667.60 m, and the lowest value is 652.29 m.

According to the specifications of the pivot model, the model's total flow rate is 326.61 $m^3 h^{-1}$ and has a supply pipe with a length of 920 m made of PVC with a nominal pipe diameter of 300 mm, which leads to the pivot point's water from a fixed level reservoir with a capacity of approximately 7000 m^3. The pumping station is composed of a pump (from the brand KSB, model WKL 150/1), with rotor 360 mm in size, which is driven by a three phase electric motor whose nominal voltage, power, and rotation values are 400V, 90 kW, and 1750 rpm, respectively. The electrical installation, with a power factor of 0.85, has electric copper cables with a length of 50 m and a cross-section of 16 mm^2.

The time of operation of the center pivot was determined to supply the water requirements of a maize crop in the study region (Domínguez et al., 2012). The gross irrigation water requirement (GIWR) applied in this period was 627 mm, with an operating time (T_o) of 1440 h.

In order to perform an economic analysis of the use of VSD in center pivot irrigation system pumping stations, the average value of 0.2 € kWh^{-1} was adopted as the reference price of the electric energy in the study region.

3. Results and Discussion

3.1. Hydraulic Model

The use of the VSPM tool made it possible to accurately characterize the irrigation system in EPANET (Figure 4). Hence, the hydraulic simulation was performed at each angular position of the center pivot lateral line, thereby obtaining the pressure distribution.

In Figure 4, two angular positions of the lateral line, 250° and 40°, are represented. These positions are those with the highest level of differences in relation to the pivot point, representing 5.68 m uphill and 9.62 m downhill, respectively.

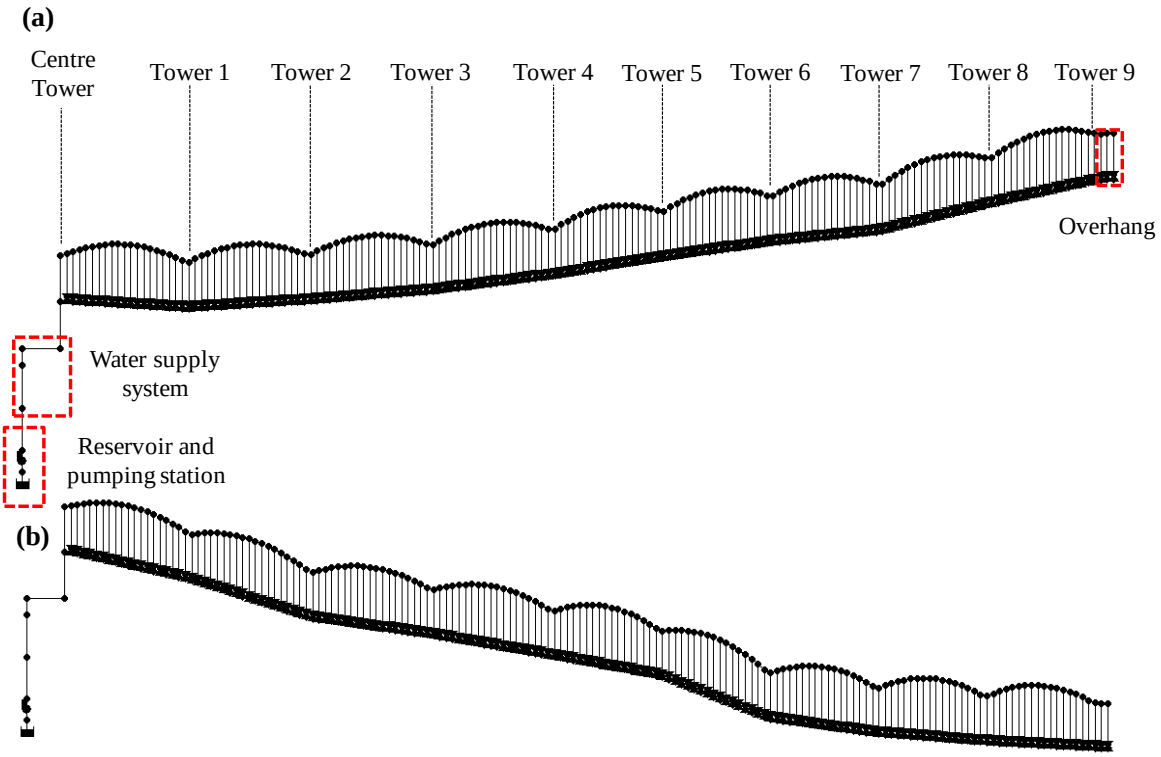

Figure 4. Network maps of the center pivot system from EPANET inp files generated by the VSPM (Variable Speed Pivot Model) tool considering two different lateral line angular positions (**a**) 250° uphill and (**b**) 40° downhill.

It can be seen that the hydraulic simulations were not performed with constant topographic slopes, as done in other works [13,20,21,24,26]. This fact allowed a greater precision in the determination of the speed of the pumping station to guarantee the lowest energy consumption with the appropriate pressurization of the lateral line in different angular positions.

The EPANET nodes and links corresponding to the fixed-level reservoir, pumping station, suction pipe, and supply pipe are highlighted in Figure 4. It should be noted that these hydraulic elements with their characteristics are constant in all angular positions of the lateral line of the center pivot. The pipe in the overhang is also highlighted in Figure 4, showing that the slope at the end of the lateral line is maintained with the same slope value of the last span. In addition, the correct characterization of the topography of the irrigated area allowed precise characterization of the energy consumption of the irrigation system operating with a maximum fixed and variable speed for the pumping station.

3.2. Operating Point

The characteristic curves of the pumping station (Q-H_P, Q-η_P, and Q-P_{Abs}), adjusted through data taken from the manufacturer, are shown in Figure 5. The operating point of the index characteristic curve "f", relative to the configuration of the pumping unit with a fixed speed is shown. In addition, the operating point of the index characteristic curve "v" refers to the configuration with a variable speed. In both cases, the angular position of the lateral line of 40° was represented with the fixed speed (n_f = 1750 rpm and α = 1.00) and variable speed pump (n_v = 1523 rpm and α = 0.85). This position was chosen because it has a minor pressure head value.

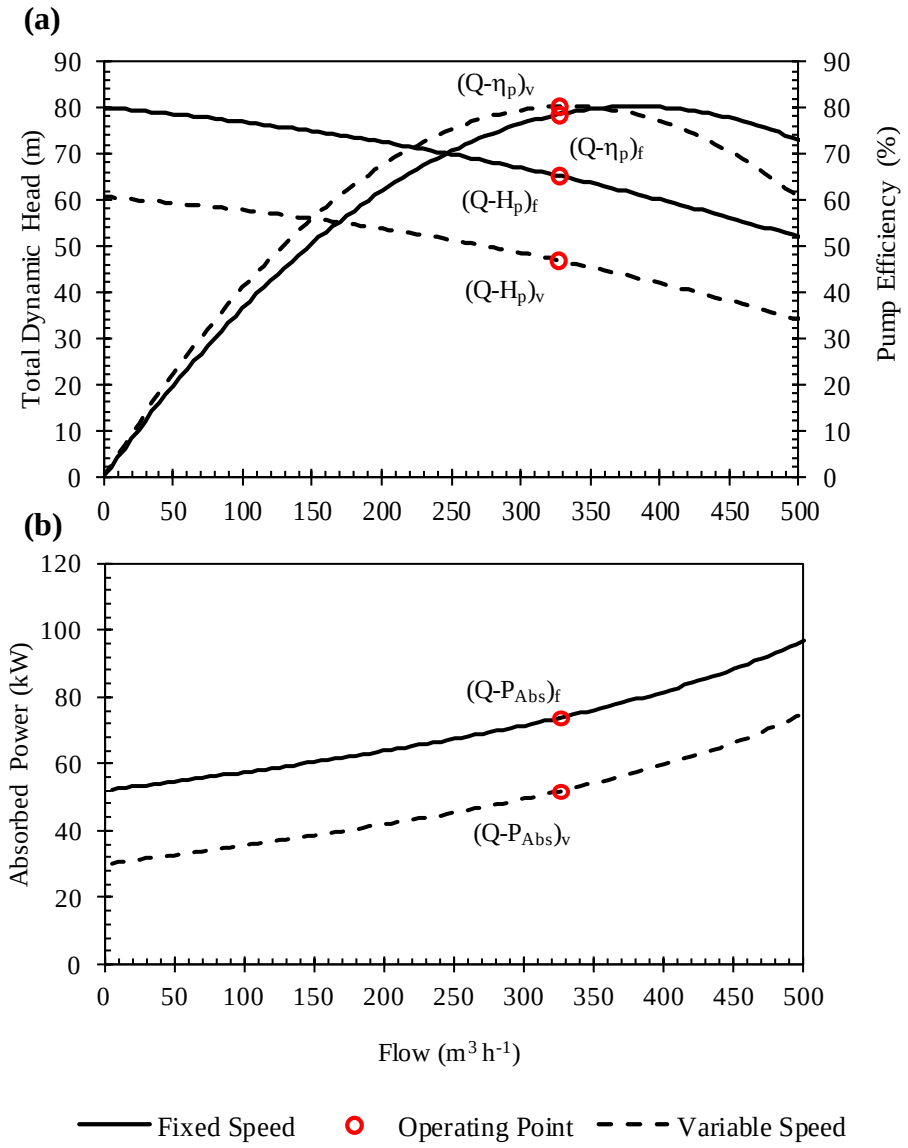

Figure 5. Pumping station characteristic curves for the 40° angular position lateral line with a fixed speed (f) and variable speed (v), (**a**) (Q-H) and (Q-η) curves, (**b**) (Q-P_{Abs}) curve.

In Figure 5, it can be seen that the displacement of curves $(Q\text{-}H_p)_v$ and $(Q\text{-}P_{Abs})_v$ to $(Q\text{-}H_p)_f$ and $(Q\text{-}P_{Abs})_f$ did not result in significant differences in pump efficiency $(Q\text{-}\eta_P)_{f,v}$. This result demonstrates that the use of the VSD in the irrigation system does not significantly interfere with the pump efficiency, whose high and low values were close to 80.26% (α = 0.85) and 78.54% (α = 1.00). This displacement also demonstrates the reduction of energy consumption (12.2%) through the influence of the VSD on the pumping station of the irrigation system under study. This same behavior of curve displacement was reported by [20] in a study on energy efficiency in center pivots. They determined that by reducing the speed of the pumping station's rotation through the VSD, it was possible to reduce its head pressure, thereby maintaining the efficiency of the pump. Also, as described by [27], the ratio (in kWh m^{-3}) can be higher at lower frequencies than the nominal value, thus presenting another source of energy saving.

3.3. Pressure Distribution Along the Lateral Line

After the hydraulic simulation of the center pivot, the pressure values at the top of the lateral line were obtained for each angular position at the nodes referring to the water outlets. Thus, the minimum pressure head value corresponds to the minor value of the pressure distribution. The pump speed computed at each angular position was the minimum pump speed that was able to keep pressure values at the downstream node of every PRV equal to the setting pressure (ie keeping every PRV at the Partially closed state). So, according to EPANET PRV rules described above, this condition was achieved when pressure values at every PRV upstream node were above the setting pressure. The minimum pressure head values and the location of the minimum pressure head along the lateral line are shown in Figure 6.

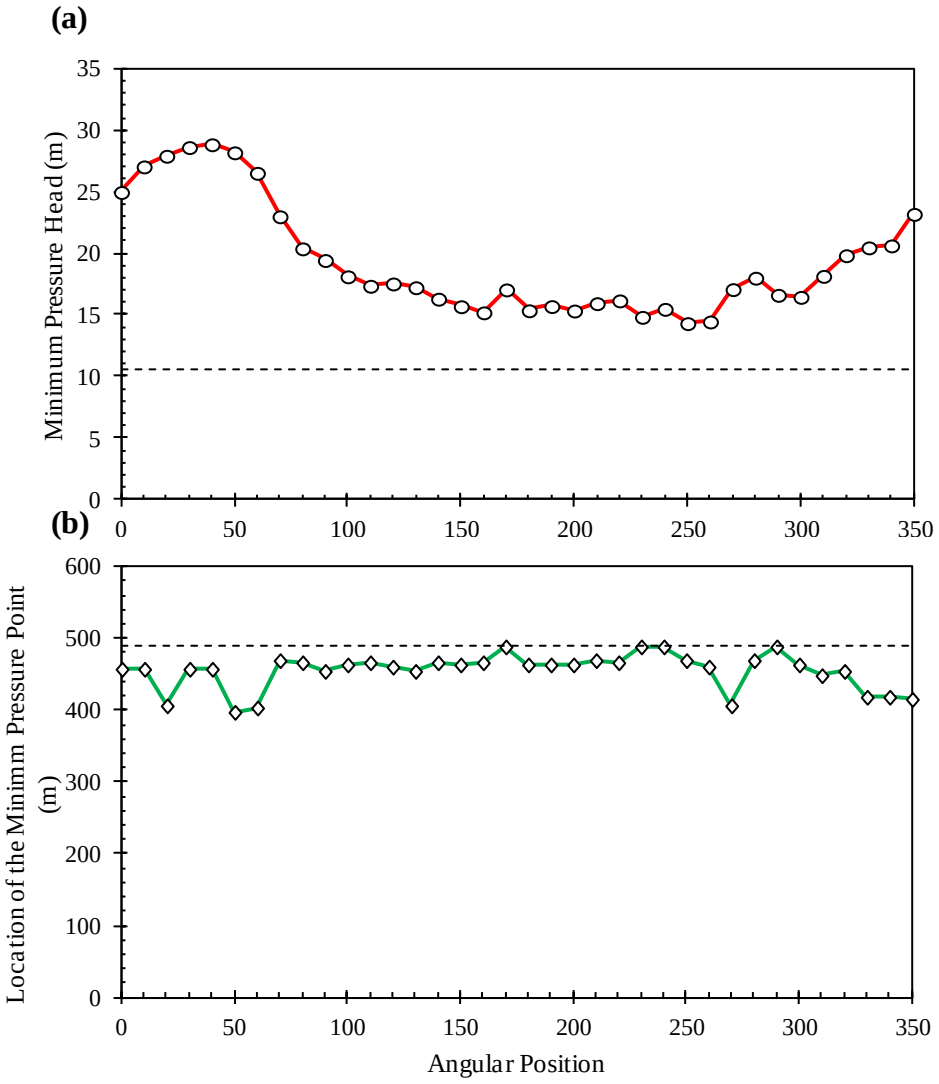

Figure 6. (**a**) Value and (**b**) location of the point of minimum pressure head in the different angular positions of the center pivot lateral line.

According to [13,20,21], the point of minimum pressure is located between the end of the lateral line and the center of the pivot according to the topographic changes of the irrigated area.

King and Wall (2000) [13], studying the spatial distribution of pressure on the lateral portion of a center pivot (with a length of 392 m and a difference in the level of 18 m), reported that the point of minor pressure on the lateral line was not necessarily situated at the end. The location of that point

was variable according to the different slopes of the irrigated area. This fact made it difficult to install pressure sensors to control the speed of the pumping station with a VSD.

Figure 6 also shows the location of the point of minimum pressure with respect to the end of the lateral line. In some angular positions, the minimum pressure value is located exactly at the end of the lateral line. This result shows the influence of the small topographic differences of the irrigated area on the location of the minimum pressure point and, consequently, on the potential reduction of energy consumption.

3.4. Energy Analysis

Pumping stations are designed for the lateral line's most critical angular position, i.e., the position where the lateral line has the largest positive level difference. Thus, the minimum pressure head is located at the lateral end. Pumping station values for the different lateral line angular positions and values for the fixed speed pump are shown in Table 1.

Table 1. Flow rate (Q), pumping pressure head (H_i), hydraulic power (P_H), speed of the pumping station (n), variable speed ratio (α), efficiencies (η), and specific energy consumption (CEE) in the different angular positions of the lateral line.

Angular Position	Q ($m^3\ h^{-1}$)	Hi (m)	P_H (kW)	n	α*	η_p (%)	η_m (%)	η_v (%)	η_c (%)	η_t [1] (%)	CEE (kWh m^{-3})
Fixed	326.61	65.23	58.04	1750	1.00	78.54	94.13		98.60	72.90	0.244*
0°	326.61	50.72	45.12	1574	0.90	80.08	93.86	96.75	98.65	71.74	0.193
10°	326.61	48.64	43.27	1547	0.88	80.20	93.77	96.21	98.66	71.38	0.186
20°	326.61	47.77	42.50	1535	0.88	80.23	93.73	95.95	98.66	71.19	0.183
30°	326.61	47.07	41.88	1526	0.87	80.26	93.69	95.71	98.66	71.01	0.181
40°	326.61	46.84	41.67	1523	0.87	80.26	93.68	95.63	98.67	70.94	0.180
50°	326.61	47.49	42.25	1531	0.88	80.24	93.71	95.86	98.66	71.12	0.182
60°	326.61	49.16	43.74	1553	0.89	80.17	93.79	96.36	98.66	71.48	0.187
70°	326.61	52.69	46.88	1599	0.91	79.93	93.93	97.13	98.64	71.93	0.200
80°	326.61	55.29	49.20	1631	0.93	79.70	94.00	97.43	98.63	72.00	0.209
90°	326.61	56.24	50.04	1643	0.94	79.61	94.02	97.48	98.63	71.96	0.213
100°	326.61	57.57	51.22	1659	0.95	79.47	94.04	97.51	98.63	71.88	0.218
110°	326.61	58.33	51.90	1669	0.95	79.39	94.05	97.50	98.62	71.80	0.221
120°	326.61	58.15	51.73	1666	0.95	79.41	94.05	97.50	98.62	71.82	0.221
130°	326.61	58.45	52.01	1670	0.95	79.38	94.06	97.50	98.62	71.79	0.222
140°	326.61	59.38	52.83	1681	0.96	79.27	94.07	97.45	98.62	71.67	0.226
150°	326.61	60.00	53.38	1689	0.96	79.20	94.08	97.41	98.62	71.58	0.228
160°	326.61	60.49	53.82	1695	0.97	79.14	94.09	97.37	98.62	71.49	0.230
170°	326.61	58.63	52.16	1672	0.96	79.36	94.06	97.49	98.62	71.77	0.223
180°	326.61	60.33	53.67	1693	0.97	79.16	94.08	97.38	98.62	71.52	0.230
190°	326.61	59.99	53.37	1688	0.96	79.20	94.08	97.41	98.62	71.58	0.228
200°	326.61	60.35	53.69	1693	0.97	79.16	94.08	97.38	98.62	71.52	0.230
210°	326.61	59.75	53.16	1686	0.96	79.23	94.08	97.43	98.62	71.61	0.227
220°	326.61	59.52	52.96	1683	0.96	79.25	94.07	97.44	98.62	71.65	0.226
230°	326.61	60.86	54.15	1699	0.97	79.10	94.09	97.33	98.62	71.43	0.232
240°	326.61	60.21	53.57	1691	0.97	79.17	94.08	97.39	98.62	71.54	0.229
250°	326.61	61.37	54.60	1705	0.97	79.03	94.10	97.27	98.61	71.33	0.234
260°	326.61	61.24	54.48	1703	0.97	79.05	94.09	97.28	98.61	71.36	0.234
270°	326.61	58.61	52.15	1672	0.96	79.36	94.06	97.49	98.62	71.77	0.222
280°	326.61	57.68	51.32	1661	0.95	79.46	94.04	97.51	98.63	71.87	0.219

290°	326.61	59.07	52.56	1677	0.96	79.31	94.07	97.47	98.62	71.71	0.224
300°	326.61	59.24	52.70	1679	0.96	79.29	94.07	97.46	98.62	71.69	0.225
310°	326.61	57.53	51.19	1659	0.95	79.48	94.04	97.51	98.63	71.88	0.218
320°	326.61	55.85	49.69	1638	0.94	79.65	94.01	97.47	98.63	71.98	0.211
330°	326.61	55.22	49.13	1630	0.93	79.71	93.99	97.42	98.63	72.00	0.209
340°	326.61	55.05	48.98	1628	0.93	79.73	93.99	97.41	98.63	72.00	0.208
350°	326.61	52.50	46.71	1596	0.91	79.95	93.92	97.10	98.64	71.92	0.199

[1] Total efficiency * variable speed drives (VSDs) efficiency not considered.

In Table 1, it can be sheen that the i = 40° position (Figure 4) has the lowest pumping pressure head value (46.84 m) and, consequently, a lower specific energy consumption value (0.180 kWh m^{-3}). On the other hand, position I = 250° presents the highest values−61.37 m and 0.234 kWh m^{-3}, respectively. It should be noted that for these positions, the determination of the CEE with the variable speed of the pump is different from the CEE with a fixed speed, because, in this configuration, the value of VSD efficiency is not considered.

Specific energy consumption (kWh m^{-3}) values for the fixed speed (without VSD) and variable speed (with VSD) pumping stations were determined. The specific energy consumption using the VSD was computed as the average values considering all the angular positions of the lateral line. In general, due to the small variations in the topography of the irrigated area, the average value of the CEE with variable speed of the pumping station was close to the value of the CEE with a fixed speed (0.214 and 0.244 kWh m^{-3}, respectively), resulting in an energy reduction value of 12.2%. This percentage is lower than the values found by [18] (32% energy savings using variable speed well pumps in a center pivot system), [19] (27% to 35% of energy savings can be achieved using VSD in two Italian irrigation districts operating with three parallel horizontal axis pumps), and higher than those found by [20] (9.6% energy reduction is possible for 13.6 m difference in the irrigated area for a study containing 100 center pivots in Nebraska (USA), with each pivot containing a pumping station). However, these studies did not take into account the efficiency of VSD. The energy reduction value of this study is close to that found by [13] (7.5% to 15.8%), who considered the variable speed drive efficiency of a center pivot pumping unit. This result demonstrates that using VSD can reduce energy consumption in pumping units for water distribution.

In the present study, the center pivot system is equipped with a single pump. The use of VSDs in situations where multiple pumps supply several irrigation systems can result in greater energy savings, as can be seen in the studies conducted by [18] and [19].

The values of the absorbed power (the relation of the hydraulic power and total efficiency, in kW) at the pumping station at each of the angular positions of the center pivot's lateral line are shown in Figure 7.

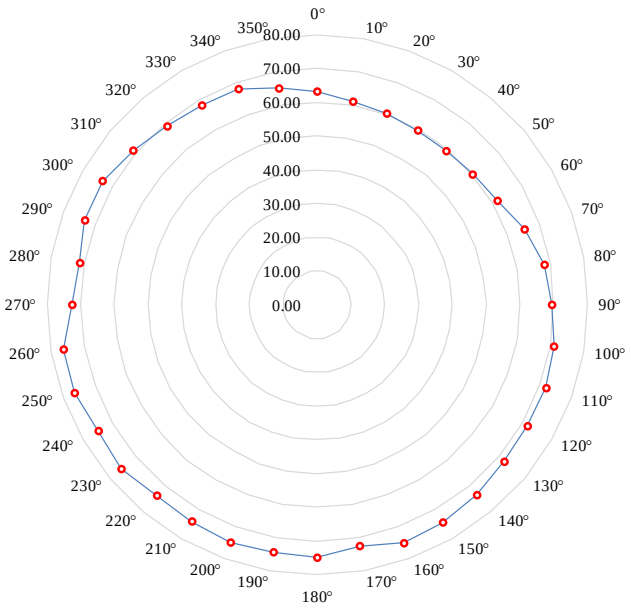

Figure 7. Absorbed power at the pumping station for the different angular positions of the lateral line.

In Figure 7, the lowest values of the absorbed power (51.92 kW) were reached in the angular positions where the lateral line assumes a downward slope (i = 40°) from the center to the end. In the same way, when the lateral line presents an ascending slope (i = 250°), it results in higher values of absorbed power (69.09 kW). This difference in values results in a reduction of 28.5% between these two angular positions. It should be noted that the total efficiency of these two positions is very close (70.9% (for i = 40°) and 71.3% (for i = 250°)). These results are directly related to the movement of the point of minimum pressure along the lateral line according to topographic variations of the irrigated area. The same type of behavior for the minimum pressure point was reported by [20] and [13] in studies with energy conservation in the center pivot systems using variable speed drives at the pumping station.

3.5. Economic Analysis

To analyze the operation costs with the use of VSDs in this center pivot, the values of energy consumption and costs, considering the two configurations (fixed and variable speed) for an irrigation season with maize crop in the region of Albacete (Spain), are presented in Table 2.

Table 2. The consumption and cost of energy for the pumping stations with fixed and variable speeds.

Crop		**Maize**
GIWR (gross irrigation water requirement)	mm	627.00
Flow rate	$m^3\ h^{-1}$	326.61
Operation time	h	1440.00
EC_f	kWh	114739.03
EC_v	kWh	100632.47
Average cost	€ $kW\ h^{-1}$	0.20
C_f	€	22947.96
C_v	€	20126.49
Energy Savings	€ $year^{-1}$	2821.47

For an irrigated area with a maximum elevation difference of 15.3 m, and considering the use of a VSD with a fixed speed, the annual average energy savings is close to 14107.35 kWh (Table 2), representing an annual average energy cost savings of 2821.47€.

In a similar study, [13] presented an average annual saving of 18100.00 kWh, applying a requirement of 635 mm of gross water irrigation and an area with an elevation difference of 18 m. They concluded that the VSD installation would not be economically viable. This result can be explained due to the low performance of the utility's equipment and the low cost of energy (0.031 kWh^{-1}) in the region where the study was conducted, which resulted in a low average annual saving (564.30 €). The average annual energy savings (kWh) presented by [13] were similar to those determined in the present study. However, due to the unit cost of energy consumption, the financial savings were lower. This fact shows that the cost of energy, besides the topography of the irrigated area, must be taken into account for this type of analysis.

Working with several center pivots for the maize crop, [20] presented an average annual saving of 4155 kWh, applying a requirement of 284 mm of gross water irrigation to an average irrigated area of 49 ha with a height difference of 13.6 m. The average pumping cost was 0.098 kWh^{-1}, resulting in average annual savings of 407.40€. The difference of the values in this study can be explained by the smaller difference in elevation, their low energy cost, and their lower gross irrigation requirements.

4. Conclusions

This study presented a proposal to vary the pressure supplied to a center pivot irrigation system according to the angular position of the lateral line by adjusting the speed of the pumping station with a variable speed drive (VSD). A model was developed to simulate the possible reduction in energy consumption when using a VSD in a center pivot pumping station in Albacete (Spain). For topographic characterization, DEMs from satellite images (with 5 × 5 m spatial accuracy) were used, and it was concluded that the topographic precision for this type of study is essential to determine the required pressure values at each angular position of the center pivot's lateral line.

The present study showed a saving of 12.2% of energy when using speed control at the pumping station in comparison with the commonly used fixed speed. This reduction in energy allowed economic savings close to 2821.47 €, in an area irrigated by a center pivot with a difference in maximum elevation of 15.3 m and the major part of the lateral line on the ascending slope.

The VSPM tool, which added topographic, hydraulic, and energy characteristics to the irrigation system, facilitated the simulation of the center pivot irrigation system in the EPANET software, along with the analyses of the use of VSD in the speed control of the pumping station. This tool demonstrates the possible financial return when using a VSD in a center pivot pumping station that operates in areas of variable topography. This center pivot represents the greater part of the irrigated area in the ascending slope during the movement of the lateral line. Therefore, for an irrigated area where the lateral line remains in a descending slope during the greater part of its rotation, the energy savings would be greater. Thus, this tool seems to be useful for users to achieve better precision in energy and economic analyses of center pivot irrigation systems.

The use of VSD to control the speed of the pumping station of the irrigation system showed a greater reduction in energy consumption when the different angular positions of the lateral line along the irrigated area were in an ascending slope. In these positions, the point of minimum pressure tends to migrate from the extremity to the center of the pivot.

This study aimed to quantify the energy saving potential of VSDs, providing irrigation producers and professionals results that show the benefits of installing VSDs in the pumping stations of center pivot irrigation systems.

Author Contributions: Conceptualization, V.B.d.S.B., M.Á.M., and J.I.C.; methodology, V.B.d.S.B., A.C., M.Á.M.,and J.I.C.; software, V.B.d.S.B., A.C., and M.Á.M.; validation, V.B.d.S.B., A.C., and

M.Á.M.; formal analysis, V.B.d.S.B., J.I.C., A.C., and M.Á.M.; investigation, V.B.d.S.B., M.Á.M., J.I.C., and A.C.; writing—original draft preparation, V.B.d.S.B., J.I.C, M.Á.M., and A.C.; writing—review and editing, V.B.d.S.B., J.I.C., and M.Á.M.; visualization, V.B.d.S.B., J.I.C., M.Á.M., and A.C.; supervision, M.Á.M.

Funding: This research was funded by the Spanish Ministry of Education and Science (MEC) grant number AGL2017-82927-C3-2-R (Co-funded by FEDER). And, this research was financed in part by the Coordenação de Aperfeiçoamento de Pessoal de Nível Superior, Brasil (CAPES), process PDSE 88881.190146/2018-01.

Conflicts of Interest: The authors declare no conflict of interest.

Nomenclature

A_c	cross-sectional area of cable (mm^2)
C_c	electrical conductivity of copper ($m\ \Omega^{-1}\ mm^{-2}$)
CEE^f	specific energy consumption, considering the pumping station with fixed speed ($kWh\ m^{-3}$)
CEE_i^v	specific energy consumption using the VSD, for each angular position i ($kWh\ m^{-3}$)
$(CEE_i^v)_{av}$	average of the specific energy consumption in the different angular positions ($kWh\ m^{-3}$)
C_{HW}	roughness coefficient of the pipe material of the Hazen-Williams equation
cosϕ	power factor
D	pipe diameter of the lateral line
DEM	Digital Elevation Model
EC	Energy Consumption (kWh)
ER	Energy Reduction (%)
GIWR	gross irrigation water requirement (mm)
h_{arc}	maximum height of the lateral line arc (m)
h_E	height of the emitter relative to the ground (m)
hf	head loss (m)
H_i	pressure head that the pump must provide for each angular position i (m)
$H_{mín(i)}$	minimum pressure along the lateral line for each angular position i (m)
H_p	pressure head at the fixed pumping speed (m)
H_{prv}	nominal pressure of the PRV (m)
H_{prv}*	PRV pressure, including the minimum regulator requirement (m)
h_T	height of moving towers (m)
i	angular position of the lateral line (0°, 10°, ..., 350°)
j	number of moving towers
k_e	emitter discharge coefficient ($m^{2.5}\ s^{-1}$)
L	equivalent length of lateral line (m)
Lb	gross irrigation depth ($mm\ day^{-1}$)

L_c	cable length (m)
L_{DP}	total length of the drop pipe (m)
L_E	spacing between emitters (m)
L_{FE}	distance between the last emitter and next tower of the span (m)
L_{IE}	spacing between the tower and the first emitter (m)
L_j	distance from the centre tower to the index tower j (m)
L_N	distance of the node referring to the water outlet in relation to the previous tower (m)
L_S	length of span (m)
N	water outlet in the span
N_O	number of water outlets in the span
P_H	hydraulic power (kW)
PNOA	Spanish National Program of aerial photogrammetry
$P_{Abs(i)}$	absorbed power (kW)
P_{Nom}	nominal power (kW)
PRV	Pressure Regulator Valve
Q	total flow rate of the irrigation system
q_x	flow of the outlet with order number x ($m^3\ h^{-1}$)
R_{inst}	radius of installation of the emitter, relative to the centre tower (m)
R_T	radius of rotation of the tower relative to the centre tower (m)
S_T	slope between towers n e n −1
Tg	rotation time (h)
T_o	operating time of irrigation system (h)
U	nominal voltage (V)
VSD	Variable Speed Drive
VSPM	Variable Speed Pivot Model
X_i^j, Y_i^j	geographical coordinates of the moving towers j (m)
$Z_{n=x}$	elevation of the node x (m)
Z_{Tn}	tower elevation posterior to node n (m)
Z_{Tn-1}	tower elevation previous to node n (m)
α	ratio between the speed of the variable speed drive and the maximum speed as a fixed speed drive
β	exponent of the pressure
γ	water specific weight ($N\ m^{-3}$)
Δh	length of the drop pipe between the lateral line and the tower (m)
η_c	cable efficiency
η_m	motor efficiency

η_p pump efficiency

η_t total efficiency of the pumping station

η_v VSD efficiency

References

1. Alexandratos, N.; Bruinsma, J. World agriculture towards 2030/2050: the 2012 revision. *Work. Pap. No. 12-03. Rome, FAO Agric. Dev. Econ. Div. (ESA).* **2012**, 153.
2. Pereira, L.S. Water, Agriculture and Food: Challenges and Issues. *Water Resour. Manag.* **2017**, *31*, 2985–2999.
3. WBCSD Water, food and energy nexus challenges. *World Bus. Counc. Sustain. Dev.* **2014**.
4. Tarjuelo, J.M.; Rodriguez-diaz, J.A.; Abadía, R.; Camacho, E.; Rocamora, C.; Moreno, M.A. Efficient water and energy use in irrigation modernization : Lessons from Spanish case studies. *Agric. Water Manag.* **2015**, *162*, 67–77.
5. AQUASTAT FAO's global water information system: Area Equipped for Irrigation. *AQUASTAT* **2014**, 2014.
6. Frizzone, J.A.; Rezende, R.; Camargo, A.P.; Colombo, A. *Irrigação por aspersão: sistema pivô central*; 1ª.; Editora UEM: Maringá, PR, Brazil, 2018; ISBN 978-85-7628-737-7.
7. Keller, J.; Bliesner, R.D. *Sprinkle and Trickle Irrigation*; Van Nostrand Reinholh: Nova York, NY, USA, New York, 1990;
8. Folegatti, M.V.; Pessoa, P.C.S.; Paz, V.P.S. Avaliação do desempenho de um Pivô Central de Grande Porte e Baixa Pressão. *Sci. Agric.* **1998**, *55*, 119–127.
9. Gilley, J.R.; Watts, D.G. Possible Energy Savings in Irrigation. *J. Irrig. Drain. Div.* **1977**, *103*, 445–457.
10. Moreno, M.A.; Planells, P.; Córcoles, J.I.; Tarjuelo, J.M.; Carrión, P.A. Development of a new methodology to obtain the characteristic pump curves that minimize the total cost at pumping stations. *Biosyst. Eng.* **2008**, *102*, 95–105.
11. Moreno, M.A.; Medina, D.; Ortega, J.F.; Tarjuelo, J.M. Optimal design of center pivot systems with water supplied from wells. *Agric. Water Manag.* **2012**, *107*, 112–121.
12. Barbosa, B.D.S.; Colombo, A.; Souza, J.G.N. de; Baptista, V.B. da S.; Araújo, A.C.S. de Energy Efficiency of a Center Pivot Irrigation System. *Eng. Agrícola* **2018**, *38*, 284–292.
13. King, B.A.; Wall, R.W. Distributed Instrumentation for Optimum Control of Variable Speed Eletric Pumping Plants with Center Pivots. *Appl. Eng. Agric.* **2000**, *16*, 45–50.
14. Kranz, W.L.; Irmak, S.; Martin, D.L.; Yonts, C.D. Flow Control Devices for Center Pivot Irrigation Systems. *Univ. Nebraska - Lincoln Extension, Inst. Agric. Nat. Resour.* **2007**, *888*, 1–3.
15. Alandi, P.P.; Pérez, P.C.; Álvarez, J.F.O.; Moreno, M.Á.; Tarjuelo, J.M. Pumping Selection and Regulation for Water-Distribution Networks. *J. Irrig. Drain. Eng.* **2005**, *131*, 273–281.
16. Khadra, R.; Moreno, M.A.; Awada, H.; Lamaddalena, N. Energy and Hydraulic Performance-Based Management of Large-Scale Pressurized Irrigation Systems. *Water Resour. Manag.* **2016**, *30*, 3493–3506.
17. Fernández García, I.; Moreno, M.A.; Rodríguez Díaz, J.A. Optimum pumping station management for irrigation networks sectoring: Case of Bembezar MI (Spain). *Agric. Water Manag.* **2014**, *144*, 150–158.
18. Hanson, B.R.; Weigand, C.; Orloff, S. Variable-frequency drives for electric irrigation pumping plants save energy. *Calif Agric* **1996**, *50*, 36–39.
19. Lamaddalena, N.; Khila, S. Energy saving with variable speed pumps in on-demand irrigation systems. *Irrig. Sci.* **2012**, *30*, 157–166.

20. Brar, D.; Kranz, W.L.; Lo, T.; Irmak, S.; Martin, D.L. Energy Conservation Using Variable-Frequency Drives for Center-Pivot Irrigation: Standard Systems. *Trans. ASABE* **2017**, *60*, 95–106.

21. Scaloppi, E.J.; Allen, R.G. Hydraulics of Center Pivot Laterals. *J. Irrig. Drain. Eng.* **1993**, *119*, 554–567.

22. Moreno, M.A.; Córcoles, J.I.; Tarjuelo, J.M.; Ortega, J.F. Energy efficiency of pressurised irrigation networks managed on-demand and under a rotation schedule. *Biosyst. Eng.* **2010**, *107*, 349–363.

23. Rossman, L.A. EPANET 2: User Manual. *Cincinnati US Environ. Prot. Agency Natl. Risk Manag. Res. Lab.* **2000**, 104.

24. Valiantzas, J.D.; Dercas, N. Hydraulic Analysis of Multidiameter Center-Pivot Sprinkler Laterals. *J. Irrig. Drain. Eng.* **2005**, *131*, 137–146.

25. Bernier, M.A.; Bourret, B. Pumping energy and variable frequency drives. *ASHRAE J.* **1999**, *41*, 37–40.

26. Alazba, A.A.; Asce, M.; Mattar, M.A.; Elnesr, M.N.; Amin, M.T. Field Assessment of Friction Head Loss and Friction Correction Factor Equations. *J. Irrig. Drain. Eng.* **2012**, *138*, 166–176.

27. Córcoles, J.; Gonzalez Perea, R.; Izquiel, A.; Moreno, M. Decision Support System Tool to Reduce the Energy Consumption of Water Abstraction from Aquifers for Irrigation. *Water* **2019**, *11*, 323.